ON THE CO NEAR-INFRARED BAND AND THE LINE-SPLITTING PHENOMENON IN THE YELLOW HYPERGIANT ρ CASSIOPEIAE

NADYA GORLOVA,[1] ALEX LOBEL,[2] ADAM J. BURGASSER,[3] GEORGE H. RIEKE,[1] ILYA ILYIN,[4] AND JOHN R. STAUFFER[5]

ABSTRACT

We report on multiepoch optical and near-infrared spectroscopy around the first-overtone rovibrational band of CO in the pulsating yellow hypergiant ρ Cas, one of the most massive stars in the Galaxy and a candidate SN II progenitor. We argue that the double cores of the CO absorption lines, which have previously been attributed to separate circumstellar shells expelled during its recurrent outbursts, result in fact from a superposition of a wide absorption line and a narrow central emission line. The CO line doubling returns over subsequent pulsation cycles, where the superposed line emission assumes its largest intensity near phases of maximum light. We find that the morphology and behavior of the CO band closely resemble the remarkable "line-splitting phenomenon" also observed in optical low-excitation atomic lines. Based on radiative transport calculations, we present a simplified model of the near-infrared CO emission emerging from cooler atmospheric layers in the immediate vicinity of the photosphere. We speculate that the kinetic temperature minimum in our model results from a periodic pulsation-driven shock wave. We further discuss a number of alternative explanations for the origin of the ubiquitous emission-line spectrum, possibly due to a quasi-chromosphere or a steady shock wave at the interface of a fast expanding wind and the interstellar medium. We present a number of interesting spectroscopic similarities between ρ Cas and other types of cool variable supergiants, such as the RV Tau and R CrB stars. We further propose a possibly common mechanism for the enigmatic outburst behavior of these luminous pulsating cool stars.

Subject headings: infrared: stars — line: profiles — shock waves — stars: atmospheres — stars: oscillations — supergiants

Online material: color figures

1. INTRODUCTION

Hypergiant ρ Cas (HD 224014) is a naked-eye variable supergiant star ($V = 4.5$ mag, $K = 2$ mag) with a long history of photovisual photometric and spectroscopic observations. It was observed with the first near-infrared (NIR; $1–3$ μm) spectrographs in the late 1970s (Lambert et al. 1981) but has been somewhat neglected since then. This paper discusses recent spectroscopic monitoring of the NIR spectrum of this remarkable hypergiant star, revealing a wealth of remarkable temporal spectral features whose interpretation remains elusive. For example, the cores of numerous strong absorption lines always appear double. The apparent line core splitting results from a static central emission component. However, in certain variability phases ρ Cas also reveals a prominent optical and NIR emission-line spectrum that can indicate a common physical origin with the central emission components of split absorption lines. An important question to further address the peculiar nature of ρ Cas' emission spectrum is therefore if the central emission lines and the prominent emission-line spectrum form in similar circumstellar conditions (e.g., at similar distances from the surface of the hypergiant with comparable geometric density distributions). Detailed spectroscopic studies of the circum-

stellar environments of cool hypergiant stars are scarce, although they are absolutely required to properly understand the physical mechanisms that can explain their uncommonly large observed mass-loss rates. For example, can the large mass-loss rates observed in F- and G-type hypergiants, such as ρ Cas (that are too cool to accelerate the radiatively line-driven winds of luminous hot stars), result from atmospheric pulsations, since their extended winds are too warm to be accelerated by dust-driven mechanisms commonly proposed in red supergiants? Can the observed properties of ρ Cas' variable emission-line spectrum be reconciled with the pulsation kinematics of the extended atmosphere and with its uncommonly large mass-loss rates?

With a spectral type of F8–G2 Ia0 ($T_{\rm eff} = 6500–7200$ K) and a luminosity of $\log L_*/L_\odot \sim 5.7$ ($R_* \simeq 400–500$ $R_\odot$), ρ Cas is one of a small sample of known yellow hypergiants in the Galaxy. In quiescent variability phases the star loses mass at a rate of few 10^{-4} $M_\odot$, which is intermediate for cool hypergiant stars, but can increase by 2 orders of magnitude during rare outburst episodes (Lobel et al. 1998, 2003). Evolutionary tracks (e.g., Lejeune & Schaerer 2001) and possible membership to the Cas OB5 association (Humphreys 1978) indicate a stellar mass of $\sim$40 $M_\odot$ and possible ages of 4–6 Myr. Observations of CNO-processed abundances in its extended Na-enriched atmosphere (Takeda & Takada-Hidai 1994) signal that this yellow supergiant has gone through dredge-up in the red supergiant stage and is presently evolving blueward. The star is about to cross the so-called atmospheric instability region in the upper H-R diagram: "the Yellow Evolutionary Void" (Nieuwenhuijzen & de Jager 1995), where due to the enormous atmospheric scale height of these massive evolved stars, coupled with a large temperature in the shell-burning layers, the effective surface acceleration essentially vanishes, producing dynamically unstable stellar atmospheres.

[1] Steward Observatory, University of Arizona, 933 North Cherry Avenue, Room N204, Tucson, AZ 85721-0065; ngorlova@as.arizona.edu, grieke@as.arizona.edu.
[2] Royal Observatory of Belgium, Ringlaan 3, 1180 Brussels, Belgium; alobel@sdf.lonestar.org.
[3] Kavli Institute for Astrophysics and Space Research, Massachusetts Institute of Technology, 77 Massachusetts Avenue, Building 37, Cambridge, MA 02139; ajb@space.mit.edu.
[4] Astrophysical Institute Potsdam, An der Sternwarte 16, 14482 Potsdam, Germany; ilyin@aip.de.
[5] *Spitzer* Science Center, California Institute of Technology, MS 314-6, Pasadena, CA 91125; stauffer@ipac.caltech.edu.

Hypergiant ρ Cas's atmospheric instability is manifested in both its quasi-periodic photometric behavior and unusual spectral variability. It normally pulsates semiregularly (Srd) with $P = 320$–500 days and an amplitude of ± 0.2 mag (V band) (Zsoldos & Percy 1991; Arellano Ferro 1985). Once every 20–50 yr, however, this hypergiant goes into an outburst by dimming more than a full visual magnitude, decreasing the effective temperature by more than 3000 K, and by ejecting a massive gas shell. The most recent outburst event occurred in 2000–2001, which was carefully monitored using high-resolution optical spectroscopy (Lobel et al. 2003). In this paper we present the NIR (2 μm) spectrum from that exceptional epoch in § 3.1.

The spectrum of ρ Cas outside the outburst is peculiar. Optical studies reveal that the spectral lines are very broad due to large atmospheric micro- and macroturbulence velocities (11 and 21 km s^{-1}, respectively). The detailed profiles of certain lines are also rather complicated. Besides the single-component weak absorption ("normal") lines that are entirely formed in the supergiant's lower photosphere, the low-excitation ($\chi_{\mathrm{low}} \lesssim 3$ eV) absorption lines are either *cyclically* or *permanently* split (depending on the line oscillator strength within a multiplet), having one component always blueshifted and the other one redshifted relative to the stellar radial velocity of -47 ± 1 km s^{-1}. A number of low-excitation lines appear in emission above the flux level of the local continuum around variability phases of maximum light (e.g., when effective temperature becomes largest), while others, such as the forbidden [Ca II] lines, always peak prominently above the local continuum level throughout a complete variability cycle. In addition, many medium-strong and strong absorption lines develop far-violet extended wings during certain phases of fast wind expansion. They can sometimes also display a rather "bumpy structure" in the far short-wavelength wing profile of split absorption lines.

Despite the fact that ρ Cas's peculiar spectrum was immediately recognized almost a century ago, its precise physical origin remains heavily debated. This is no surprise given that it requires an appreciable amount of observing time to acquire the substantial body of simultaneous spectroscopic and photometric data necessary to reveal a correlated pattern of behavior. The earliest interpretations of the peculiar line splitting phenomenon attribute it to two detached circumstellar shells previously ejected by the supergiant (Bidelman & McKellar 1957; Sargent 1961; Gesicki 1992). Various authors remarked that such shells possibly comprise two atmospheric layers flanking an outwardly propagating shock wave, a mechanism currently used to explain the absorption-line splitting observed in a number of less luminous variables such as RR Lyr, W Vir, RV Tau, and Miras (e.g., Chadid & Gillet 1996; Whitney 1962; Gillet et al. 1989; Hinkle et al. 1982). Sheffer & Lambert (1986) added support to the shock wave hypothesis for ρ Cas by showing that the line core doubling correlates with the pulsation phase, because the splitting is most prominent around maximum light when the photosphere begins to expand. They also argued that the line core doubling first starts in the high-excitation lines, as if a shock wave were propagating outward crossing various atmospheric regions with decreasing χ_{low}. However, Sheffer (1993) also considered a different explanation for the split lines of ρ Cas. Instead of two separate absorption components, the splitting could be interpreted as a superposition of a single broad absorption line and a static central *emission* line. This proposition was based on the observation of the cores of some split lines that become so intense at times that they peak above the local level of the continuum, sometimes without any accompanying absorption, which also rules out a P Cygni–type line formation region in ρ Cas. These effects were also noted for

the slightly warmer hypergiant HR 8752. The emission can be better detected against the weaker absorption spectrum of this hypergiant (Sheffer & Lambert 1987). Sheffer & Lambert (1987) hence proposed that the origin of the variable emission lines could be in a putative extended chromosphere around these very luminous cool stars.

Further steps at discarding the "shell hypothesis" for the formation of split absorption lines in ρ Cas were provided in Lobel et al. (1998). They showed that (1) the observation of *permanently* split absorption lines in the optical spectrum, with components remaining at a constant radial velocity, would require two absorbing "shells" moving with positive and negative radial velocity during the complete variability cycle. Two separate shells permanently propagating in opposite directions is physically excluded; (2) the high-excitation lines considered in Sheffer & Lambert (1986) do not necessarily form deeper than low-excitation lines in the extended atmosphere of ρ Cas and therefore do not provide additional "evidence" for an outwardly propagating atmospheric shock wave; and (3) the variations of the red- and blueshifted components in the split absorption lines are not independent of each other. One line component always grows stronger, while the other line component weakens. This effect can readily be mimicked by assuming a central static emission line superimposed on a stronger and broader absorption line that exhibits small Doppler displacements due to the photospheric oscillations. Further direct evidence against substantial circumstellar material around ρ Cas includes the nondetection by the *Hubble Space Telescope* Wide Field Planetary Camera 2 of any significant structure at 0″.1 or 310 AU $\approx 150 R_*$ away from the hypergiant (Schuster et al. 2006). Nevertheless, tenuous and temporal circumstellar material may still be present, as indicated by a weak mid-IR excess (Jura & Kleinmann 1990) and the spectroscopically observed mass ejections during recurrent outbursts of the star (e.g., optical TiO band observations by Lobel et al. [2003] and references therein to the two earlier recorded outbursts).

In this paper we address the important question of the origin and nature of the line emission region in ρ Cas. In particular, what are its thermal conditions, and what is the geometric extension and location of this region? Can the emission region and its line excitation mechanism be linked to the pulsations of the lower photosphere of the hypergiant? We discuss several important clues from NIR spectra of ρ Cas but also scrutinize new high-resolution optical and UV observations (of which a more detailed analysis will be presented elsewhere).

While optical TiO bands have only been recorded during rare outbursts, the abundant CO molecule is, however, always observed in the NIR spectrum of ρ Cas. The NIR spectrum was extensively monitored by Sheffer (1993) with the Fourier Transform Spectrograph (FTS) on the Mayall 4 m telescope (Kitt Peak) from 1979 to 1989. Their intense monitoring program revealed substantial NIR spectral changes on a timescale of only months (Sheffer 1993). Although the shell hypothesis can be abandoned for the optical split absorption lines, these authors adopted it to interpret the CO line variability in the NIR spectrum. Unlike the optical atomic split lines, the NIR CO lines require kinetic gas temperatures much smaller than those adopted in classical photospheric models for F- and G-type supergiants (for a comprehensive CO Grotrian diagram, see Fig. 1 of Bieging et al. [2002]). The low kinetic gas temperatures ($\lesssim 2000$ K) required for CO molecular formation at these early spectral types either require a temperature reversal in the upper atmosphere (a model we explore in § 4.2) or must assume the presence of a much cooler circumstellar gas envelope. The latter interpretation was adopted

by Sheffer (1993) by attributing the short-wavelength shell component of the split CO absorption lines to a moderate outburst of ρ Cas in 1986. They further assumed the detached shell interpretation to compute the total mass of the expelled gas layer, its turbulent velocity, and the atmospheric deceleration during their monitoring period.

NIR CO bands have been observed and interpreted as direct tracers of ejected stellar material in a number of other F–G supergiants. For example, Oudmaijer et al. (1995) discussed the molecular winds of post-AGB stars, while Gonzalez et al. (1998) investigated dust formation close to the stellar surface of R CrB stars. Given the difficulties of properly explaining the properties of split *atomic* lines in ρ Cas, we argue that a shell hypothesis for CO line formation needs to be reexamined as well. The early investigations by Sheffer (1993) already indicated that, despite the wide variety of morphologies exhibited by the CO line profiles, they can nonetheless be reduced to a narrow central emission line superimposed on a broad absorption line, yielding two adjacent (but therefore only "apparent") absorption-line components. However, their study was not widely published or discussed, and only one FTS spectrum has been discussed by Lambert et al. (1981). The major part of these exceptional NIR spectroscopic data were only presented as part of a Ph.D. thesis (Sheffer 1993).

We present a collection of NIR spectra of ρ Cas obtained with several telescopes in 2000–2004. Our NIR monitoring program is not as frequent as Sheffer's (1993) but has the following benefits. First, we present spectral analyses of new NIR observations in combination with our ongoing optical high-resolution spectroscopic monitoring of ρ Cas since 1993 (Lobel et al. 2003). Next, while Sheffer et al. studied NIR spectra of the moderate outburst of 1986, we investigate the major outburst event of 2000–2001. Following the latter major outburst, the long-term variations in Hα reveal the formation of an exceptional P Cygni–type line profile since the spring of 2004 (Lobel 2004; Lobel et al. 2006). Cool supergiant stars often exhibit secular variations on timescales of decades (for examples, see § 5.2.1), and it is therefore important to continue accumulating spectroscopic observations of these unusual stars.

Although our combined spectra span the entire range from optical wavelengths longward of Hα through the main NIR J, H, and K bands, up to L (4 μm), the present study primarily concentrates on the K-band region where the first-overtone band of CO occurs (§ 3). Our high-resolution CGS4 spectral observations of 2004 September are motivated by the large variability of this molecular band observed in low-resolution spectra, and because it was detected in strong emission in 1998. We also draw attention to the L-band region in the SpeX spectrum (§ 3.1) because, to our knowledge, it is the first L-band spectrum of medium spectral resolution presented for any F-type supergiant, such as ρ Cas.

The outline of this paper is as follows. First we describe new optical to NIR spectra of ρ Cas obtained in 1998–2004, covering roughly four pulsation cycles (§ 2). Then we establish the presence of emission in NIR CO lines and investigate their profile changes with the stellar pulsations (§ 3). We discuss a unified excitation mechanism that can produce emission in both molecular and atomic lines, considering several explanations based on detailed CO line modeling, combined with coeval optical spectroscopy (§ 4). Finally, we compare our observations with the line-splitting phenomenon reported in other cool star spectra. For example, we show that the brightness declines of R CrB stars appear intriguingly similar to the outbursts of ρ Cas (§ 5). The comprehensive approach of our NIR monitoring program enables us to investigate the remarkable evolution of the CO 2.3 μm band

and to provide credible evidence for the stellar pulsations as the dominant factor that determines the profile changes observed in NIR and optical low-excitation spectral lines (§ 6).

2. OBSERVATIONS AND DATA REDUCTION

2.1. *IR Spectroscopy*

We have collected a series of low ($R \sim 300$) to high ($R \sim$ 40,000) spectral resolution NIR spectra of ρ Cas covering roughly four pulsation cycles in 1998–2004. Our observations use three instruments on three telescopes: the CorMASS echelle spectrograph on the 1.9 m Vatican Advanced Technology Telescope in Arizona (Wilson et al. 2001), the SpeX echelle spectrograph on the 3 m Infrared Telescope Facility (IRTF; Rayner et al. 2003), and the CGS4 spectrograph on the 3.8 m United Kingdom Infrared Telescope (UKIRT; Mountain et al. 1990) at Hawaii. Observations with the latter spectrograph were obtained in service mode. The data sets are complemented with two archival CGS4 spectra: one obtained in 1998, one pulsation cycle before; and the other one right in the middle of the grand outburst minimum of 2000–2001. Table 1 summarizes all observing dates and the basic characteristics of the new NIR spectra.

All NIR observations are performed in a standard fashion resulting in similar data reduction procedures. A series of successive A–B sequences (where A and B correspond to two positions of the star along the slit) are obtained, both for ρ Cas and a bright telluric standard A-, F-, or G-type star. Exposure times range from 0.5 to 2 s, usually restricted to the shortest time allowed for a particular instrument. The size of the entrance slit ranges from 0″.3 to 2″, the allowed minimum to attain maximum available spectral resolution. To suppress the brightness of ρ Cas before saturation, a neutral density filter is used with CorMASS and for the low-resolution mode of CGS4 (both for ρ Cas and telluric standards).

The flat-fielded A and B images are combined and mutually subtracted to perform dark and sky removal. The spectral orders are extracted, wavelength-calibrated, and divided by a standard star spectrum with removed intrinsic hydrogen lines. Next, they are trimmed and combined into a single NIR spectrum. The resulting spectrum is then multiplied by a blackbody spectrum corresponding to the spectral type of the standard. The wavelength calibration of the CorMASS spectra is performed using observations of the planetary nebula NGC 7027 obtained during the same night or the night before. The calibration of the high-resolution CGS4 spectra and the short-wavelength mode of SpeX employ Ne-Ar-Xe arc lamp exposures obtained immediately after science target observation. The low-resolution CGS4 observations and the SpeX long-wavelength mode calibration both employ these arc lamp exposures as well as extraction of sky lines from the target images. An accurate absolute flux calibration has not been attempted for the obvious reasons of intentional flux suppression and strong seeing-induced variations between subsequent exposures of this very bright star.

A number of important differences in our reduction procedures using different instrument/grating settings are the following. The 40 line mm^{-1} CGS4 observations require one additional step of correcting for a 2–3 pixel-wide wiggle in the flux level introduced by variations in the seeing conditions. It occurs when the detector is shifted in the dispersion direction between subsequent exposures to improve the sampling of the resolution element on the detector array. The basic steps for reduction of the calibration frames and co-addition of the target frames are performed with the ORAC-DR pipeline for the CGS4 low-resolution spectra. The SpeXtool software package is used for the SpeX data,

TABLE 1
Log of Spectroscopic Observations

Observing Date	Julian Date (2,400,000+)	Telescope-Instrument	Grating	Wavelength Range[a] (μm)	Resolution		Telluric Standard		Observers[b]
					$\lambda/\Delta\lambda$	(km s^{-1})	HD Number	Spectral Type	
1998 Oct 21	51,108	UKIRT-CGS4	40 line mm^{-1}	1.820−2.450	850	350	195295	F5 Iab	J. B., G. F.
2000 Jul 19	51,744	WHT-UES	E31	0.4050−0.8800	50000	6			A. L.
2000 Oct 18	51,836	UKIRT-CGS4	150 line mm^{-1}	2.040−2.114	6400	50	221756	A1 III	C. D.
2000 Oct 18	51,836	UKIRT-CGS4	150 line mm^{-1}	2.115−2.194	6700	45	221756	A1 III	C. D.
2000 Oct 18	51,836	UKIRT-CGS4	150 line mm^{-1}	2.192−2.353	3500	85	170296	A1 IV/V	C. D.
2000 Oct 19	51,837	UKIRT-CGS4	150 line mm^{-1}	2.035−2.112	6400	50	221756	A1 III	C. D.
2000 Oct 19	51,837	UKIRT-CGS4	150 line mm^{-1}	2.113−2.192	6700	45	221756	A1 III	C. D.
2000 Oct 19	51,837	UKIRT-CGS4	150 line mm^{-1}	2.189−2.352	3500	85	221756	A1 III	C. D.
2003 Jun 10	52,800	NOT-Sofin	Cam2	0.4251−0.7744	80000	4			A. L., I. I.
2003 Nov 20	52,964	VATT-CorMASS	40 line mm^{-1}	0.650−2.500	300	1000	4614	G0 V	N. G., N. W.
2004 Apr 6........	53,101	NOT-Sofin	Cam2	0.4170−0.9690	80000	4			A. L., I. I.
2004 Jul 29	53,217	NOT-Sofin	Cam2	0.3465−1.024	80000	4			A. L., I. I.
2004 Sep 6........	53,255	IRTF-SpeX	ShortXD	0.805−2.400	2000	150	205314	A0 V	A. B.
2004 Sep 6........	53,255	IRTF-SpeX	LongXD1.9	1.910−4.104	2500	120	223386	A0 V	A. B.
2004 Sep 16......	53,265	UKIRT-CGS4	40 line mm^{-1}	1.870−2.504	900	350	219290	A0 V	S. L.
2004 Sep 17......	53,266	UKIRT-CGS4	Echelle	2.1584−2.1729	37000	8	219290	A0 V	C. D.
2004 Sep 17......	53,266	UKIRT-CGS4	Echelle	2.1994−2.2131	37000	8	219290	A0 V	C. D.
2004 Sep 17......	53,266	UKIRT-CGS4	Echelle	2.2893−2.3034	37000	8	219290	A0 V	C. D.
2004 Sep 17......	53,266	UKIRT-CGS4	Echelle	2.2994−2.3134	37000	8	219290	A0 V	C. D.
2004 Sep 17......	53,266	UKIRT-CGS4	Echelle	2.3094−2.3232	37000	8	219290	A0 V	C. D.
2004 Oct 23	53,302	Mayall-ECHLR	Echelle	0.5255−0.8523	42000	7			J. S.
2004 Oct 30	53,309	VATT-CorMASS	40 line mm^{-1}	0.650−2.500	300	1000	4614	G0 V	N. G., J. G.
2004 Oct 31	53,310	VATT-CorMASS	40 line mm^{-1}	0.650−2.500	300	1000	4614	G0 V	N. G., J. G.
2004 Nov 27.....	53,337	NOT-Sofin	Cam2	0.3545−0.9875	80000	4			A. L., I. I.
2004 Dec 25	53,365	NOT-Sofin	Cam2	0.3580−1.0325	80000	4			A. L., I. I.

[a] Air wavelengths, as observed.

[b] J. B. = J. Buckle; G. F. = G. Fuller; A. L. = A. Lobel; C. D. = C. Davis; I. I. = I. Ilyin; N. G. = N. Gorlova; N. W. = N. Woolf; A. B. = A. Burgasser; S. L. = S. Leggett; J. S. = J. Stauffer; J. G. = J. Greissl.

which also performs the extraction of the final one-dimensional spectra (Vacca et al. 2003; Cushing et al. 2004). The CorMASS spectra are reduced with the standard IRAF software package `imred.echelle`. The SpeXtool routine Xtellcor provides a modified spectrum of Vega to perform telluric corrections in the SpeX spectra. For all other cases, strong hydrogen lines in the standard spectra are interpolated with a straight line and removed using the IRAF task `splot`.

2.2. *Optical Spectroscopy*

In order to investigate correlations between the behavior of CO lines, the photosphere, and the circumstellar components observed in atomic lines, we complement Table 1 with seven high-resolution optical echelle spectra obtained during our continuous monitoring program of the star in 2000−2004 (§ 5.1).

The spectrum of 2000 July 19 was observed during the deep outburst minimum with the Utrecht Echelle Spectrograph on the 4.2 m William Herschel Telescope (Canary Islands, Spain). The nominal wavelength resolution is $R \simeq 50,000$, with continuum signal-to-noise ratios (S/Ns) exceeding 100. For more detailed discussions about calibration procedures and a thorough analysis of the outburst spectra, we refer to Lobel et al. (2003).

The spectrum of 2004 October 23 was observed to follow up our CGS4 NIR observations of 2004 September that revealed strong CO emission. It was obtained 5 weeks later, and about a week before the CorMASS NIR observations, when the remarkable CO emission had already started to decrease. The spectrum was obtained with the Kitt Peak National Observatory (KPNO) 4 m Mayall telescope using the echelle spectrograph configured to provide $R \approx 40,000$ in the red (6000−8500 Å in 22 orders).

The wavelength calibration was performed with the Th-Ar lamp spectra, with a small additional shift in the zero point as inferred from terrestrial O_2 lines.

The other optical echelle spectra of 2003−2004 were observed with the Sofin spectrograph on the 2.6 m Nordic Optical Telescope (La Palma, Spain). The spectra are observed with the medium-resolution Camera 2 ($R \simeq 80,000$) with a wavelength range covering about 5000 Å over 42 echelle orders. Each observation combines a number of subsequent exposures with two central wavelength settings until a minimum S/N of $\sim$50 is reached. The S/Ns for the echelle orders centered on the CCD can therefore exceed 300 in the wavelength region of the spectral lines of interest. Typical effective exposure times are limited to 10 minutes per exposure to avoid CCD saturation for this optically bright star. Note, for example, that the large brightness of ρ Cas allows us to integrate high-quality optical spectra during dusk or dawn (i.e., at the beginning or end of a bright night run) with large zenith distances ($\geq 50^\circ$). For some of our spectra it yields large air masses (e.g., $\sim$1.6 for 2004 December 25) with strongly contaminating telluric lines, but that otherwise do not influence our spectral regions of interest. The Sofin spectra are calibrated with Th-Ar lamp spectra observed after each science exposure. The standard echelle reduction steps are performed using the 4A data acquisition and reduction software package described in Ilyin (2000). Special consideration is given to the removal of scattered light inside the spectrograph, and to the extraction of spectral orders including the removal of cosmic spikes. The wavelength dispersion solutions yield mean accuracies better than ± 1 km s^{-1}. The echelle spectra are not calibrated in an absolute flux scale, but special care is taken to apply the required
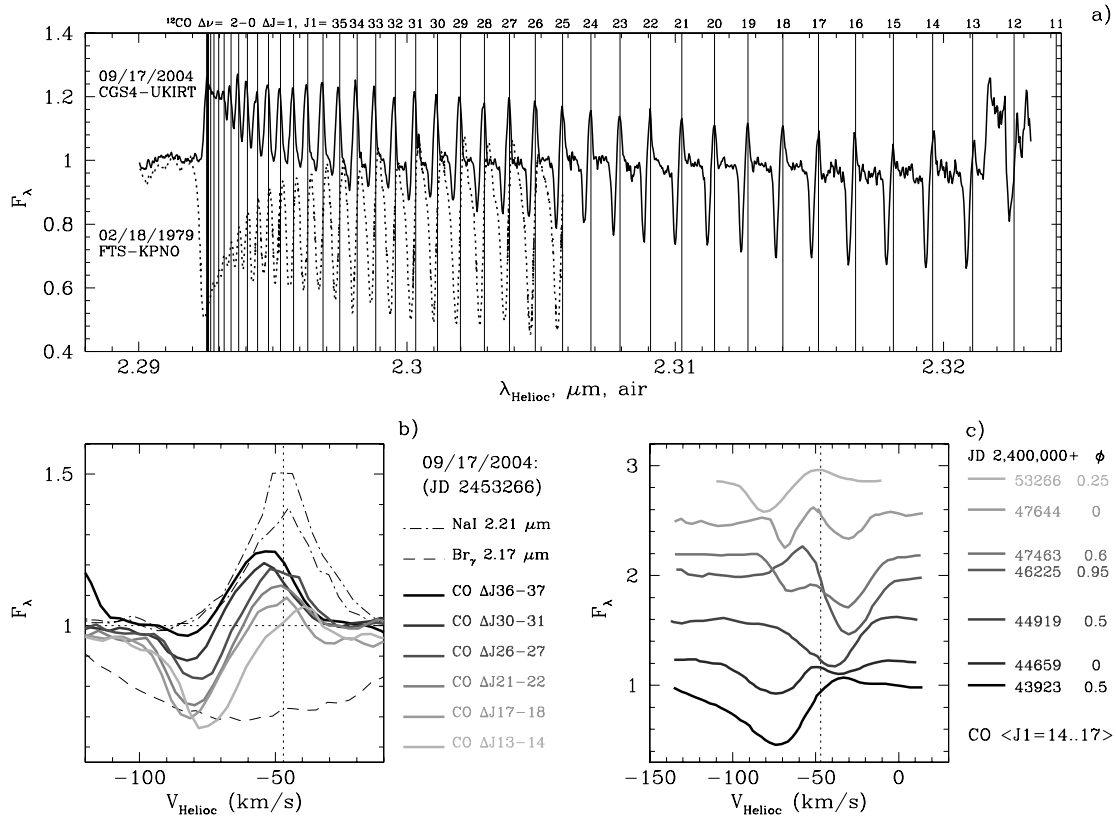
Fig. 5.—(a) High-resolution spectra of ρ Cas of the first-overtone $\Delta\nu$ 2–0 CO band observed in emission in 2004 September (*solid line*) and in absorption in 1979 February (*dotted line*; from Lambert et al. 1981). (b) Separate rotational CO transitions of 2004 September overplotted in the velocity scale, together with Na I and Brγ lines observed on the same night. (c) Averaged line profiles of the R14–R17 CO transitions from 1979 to 1989 observed by Sheffer (1993) compared to our observations in 2004. The spectral resolutions are 9 and 8 km s^{-1}, respectively. The star velocity of -47 km s^{-1} is marked with the vertical dashed line. The spectra have been continuum normalized and shifted in the vertical direction. The pulsation phases are roughly determined from the light curve in Fig. 4, with $\phi = 0.0$ corresponding to maximum brightness and $\phi = 0.5$ corresponding to minimum brightness.

A detailed comparison of the two CO spectra observed 25 yr apart reveals a striking transformation from deep absorption lines in 1979 to apparent P Cygni profiles in 2004. As indicated by our low-resolution spectra, the transformation from absorption to emission actually occurs on a regular basis every pulsation cycle. Sheffer's long-term high-resolution NIR monitoring of ρ Cas offers a unique opportunity to investigate its causes by tracking the detailed evolution of the CO line profiles. Figure 5c shows a wide diversity in line shapes exhibited by CO in 1979–2004. For a full set of profiles, we refer to Figures 5.15 and 5.16 of Sheffer (1993). When we correlate them with the corresponding pulsation phases and compare with optical line profiles, a coherent interpretation can, however, be proposed.

First, the variations of both emission and absorption-line fluxes are larger when the amplitude of the light curve (ΔV) is also larger. Compare, for example, the strong CO lines observed in 1979–1981 and 2000–2004 with the 1987–1989 epoch when the CO absorption lines remain permanently split. During the latter epoch pulsations are weak (see Fig. 4), and the two absorption-line components vary only slightly in intensity and Doppler shifts. Second, prominent CO line emission only occurs near phases of maximum light. It is always centered within ± 10 km s^{-1} around the star velocity. On the other hand, the CO line absorption can be either red- or blueshifted, with shifts of $\lesssim 30$ km s^{-1}. The precise dependence of absorption on the corresponding pulsation phase, however, remains unclear. This is in part because the CO line absorption obviously becomes filled in with variable emission. The outer atmosphere of ρ Cas is also velocity stratified and only loosely coupled to the pulsations of its lower photosphere,

which can yield different Doppler displacements for the CO absorption and emission-line formation regions. Finally, it is important to point out that the properties and the timescale of these CO line profile variations closely resemble the profile evolution observed in optical atomic split lines such as the Fe I λ5506 line in Figure 2 of Lobel et al. (2003). When one of the split absorption components strengthens, the other one weakens. The double CO core profiles can thus simply be interpreted as one broad absorption line with semiregular Doppler displacements, in which core splitting occurs when it passes across a static central emission reversal inside the line core.

The broad range of NIR CO line morphologies in ρ Cas argues firmly against a P Cygni line profile formation region. The CO emission flux varies on timescales directly linked to the variability cycles of the photospheric absorption spectrum. This is unlike classical P Cygni profiles observed in ultraviolet resonance lines of hot stars that are static and almost invariable in time. It signals that the major portion of the CO emission-line formation region is influenced by the recurrent photospheric changes in ρ Cas, rather than, for example, emission emerging from a very far extended optically thin circumstellar envelope that produces redshifted photons by backscattering in the far-side expanding hemisphere. The 2.3 μm CO emission can therefore not emerge from a (possibly) very extended molecular (e.g., CO) gas envelope around the supergiant. This is further evidenced by NIR CO line profiles observed in HR 8752, another variable cool hypergiant. Sheffer (1993) observed that either only emission occurs in its CO lines, or that it is accompanied by *redshifted* absorption, yielding an *inverse P Cygni–type* profile instead (Lambert et al. 1981). The
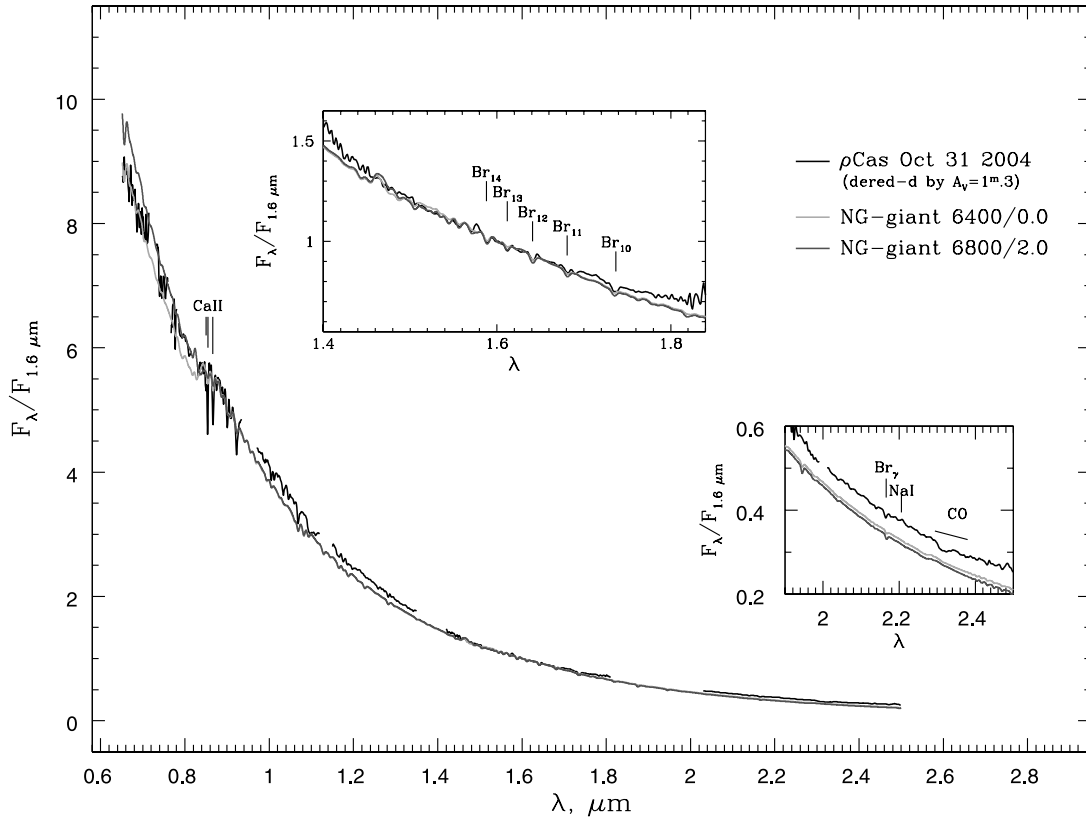
Fig. 6.— Spectral energy distribution in the low-resolution CorMASS spectra used to constrain the photospheric parameters of ρ Cas, together with the temperature-sensitive hydrogen lines and the gravity-sensitive Ca II lines. The graph shows the best-fit model spectra from the NextGen-giant grid to the spectrum of 2004 October. The strong calcium triplet lines favor the lowest gravity value of 0.0, for which models with only $T_{\rm eff} \leq 6400$ K are available. NIR CO is not expected to form in this temperature range, confirming our calculations using Kurucz model atmospheres (see § 4.2).

2.3 μm CO feature, however, vanished in HR 8752 in the late 1980s, approximately at the same time when its optical variability became much smaller and the effective temperature increased (§ 5.2.1). We now investigate where the CO emission-line formation region is located in ρ Cas.

4. MODELING CO EMISSION

Since the 2.3 μm CO band is not observed in normal F–G type supergiants, neither the CO emission nor the absorption components appear to be of photospheric origin in ρ Cas. The supergiants of our comparison sample, however, have smaller luminosities with larger gravity, and molecular bands can be strongly gravity dependent (Kleinmann & Hall 1986; McGovern et al. 2004). Furthermore, since ρ Cas is a pulsating star, can the strong variability of the underlying photospheric spectrum cause apparent variability in CO, as well as in other "external" spectral lines? The strong correlation of the CO emission flux with variability phase signals its formation close to the pulsating photosphere. We therefore adapt a numerical model of the average photosphere to probe a number of spectral properties of the CO band observed in the high-resolution CGS4 data.

4.1. *Photospheric Parameters*

Every pulsation phase of ρ Cas requires an estimate of at least two photospheric model parameters: effective temperature and $\log g$. We first compare the CorMASS spectra of ρ Cas with its less luminous cousins: the Cepheids and the nonvariable yellow supergiants of our sample. In the latter stars the photospheric lines are sufficiently narrow to apply the classical method of

absorption-line depth ratios to reliably infer the effective temperature. Figure 1 shows two spectra of the 3 day period classical Cepheid Y Aur obtained about half a pulsation cycle apart. High-resolution optical spectroscopic studies show that the effective temperature of short-period Cepheids can vary between 5500 and 6500 K with $\log g = 1.9$–2.3 (Kovtyukh & Gorlova 2000). For the early G nonvariable μ Per in Figure 1 we adopt $T_{\rm eff} = 5330$ K and $\log g = 1.8$ (V. Kovtyukh 2005, private communication). When comparing CorMASS spectra of ρ Cas of 2003 November and 2004 October to Y Aur and μ Per, we find that the effective temperature should exceed 5500 K for ρ Cas. To get a better constraint on the temperature, we fit the CorMASS spectra of ρ Cas (after dereddening by $A_V = 1.3$ mag; Zsoldos & Percy 1991) with the NextGen-giant model spectra computed with the Phoenix code (Hauschildt et al. 1999). Our best fits confirm a $\log g$ value of ~0.0, whereas for the effective temperature only a lower limit can be derived due to a lack of models with $T_{\rm eff} \geq$ 6600 K and $\log g < 2.0$ (Fig. 6). We obtain a $T_{\rm eff} \geq 6400$ K for the spectrum of 2003 November, but slightly cooler for 2004 October. The light curve (Fig. 4) shows that the star assumes maximum brightness between 2003 November and 2004 October. The star is dimmer in the V band in 2004 October compared to 2003 November, which confirms the smaller effective temperature derived from our best-fit procedure. If one assumes that the CO absorption component forms in the photosphere and becomes stronger with smaller effective temperature, then the shallower CO absorption band observed in 2004 October must result from filling in by emission, which occurs on the descending branch of the light curve. In § 4.2 we investigate whether or not the CO absorption component forms in the stellar photosphere.
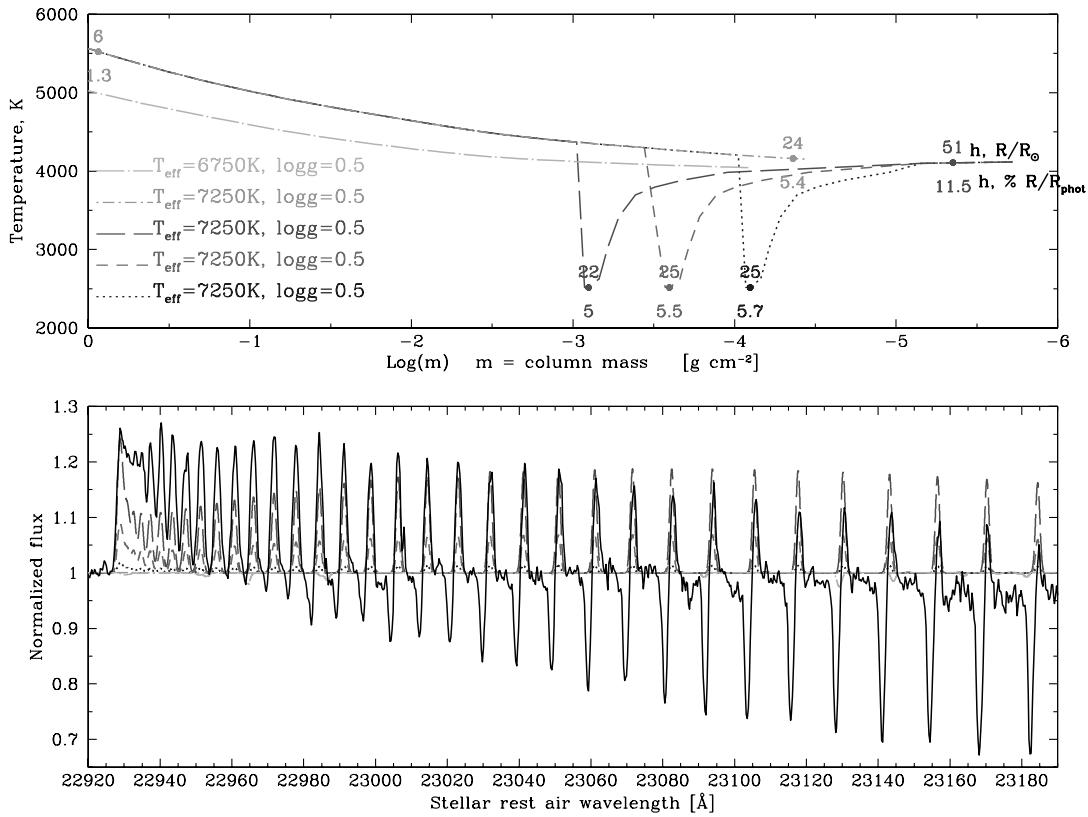
FIG. 7.—*Top:* Atmospheric gas temperature structures used to calculate the model spectra. The horizontal axis is in the column mass scale m. The outer layers of the atmosphere correspond to smaller values of $\log m$. The marked numbers on the atmospheric temperature profiles show the corresponding geometric scale expressed as the height above the photosphere (where by definition the optical depth $\tau = 2/3$ and $T_g = T_{eff}$) in solar radius (*top row*) and in percent of the photospheric radius (adopting $R_* = 450\ R_\odot$ for ρ Cas; *bottom row*). *Bottom:* CGS4 high-resolution spectrum of ρ Cas of 2004 September (*solid line*) plotted against synthetic model spectra calculated with temperature structures in the top panel. The model spectra are blueshifted by 7 km s^{-1} to match the velocity of the observed CO band head. Dot-dashed spectra are calculated using Kurucz atmosphere models, while the long-dashed, short-dashed, and dotted models include a cool gas layer in the upper atmosphere at $\log m = -3, -3.5$, and -4, respectively. The model adapted with a temperature minimum at $\log m = -3$ best fits the observed emission flux around the CO band head. None of the adapted models yield significant NIR CO absorption. [*See the electronic edition of the Journal for a color version of this figure.*]

We can also constrain the effective temperature from our high-resolution *optical* spectra. Lobel et al. (2003) established a tight relationship between the equivalent width (EW) of the Fe I $\lambda5572$ absorption line and the effective temperature of ρ Cas. Our optical echelle spectrum of 2004 April 6 indicates an EW for the Fe I line of 348 mÅ, which corresponds to $T_{eff} = 7290$ K. In the spectrum of 2004 October 23 we measure an EW = 465 mÅ, yielding $T_{eff} = 6910$ K. In addition, the visual brightness in 2004 October was comparable to 2003 June, for which Fe I provides $\sim$6800 K. These estimates agree well with the lower limits estimated from the CorMASS spectra. They confirm that the hypergiant was cooling down while dimming to minimum brightness (after early spring 2004), but it did not cool to below 6000 K. We can hence adopt a reliable estimate of $T_{eff} = 7200 \pm 100$ K for the SpeX and CGS4 emission spectra of 2004 September, and of 6800 ± 100 K for the CorMASS absorption spectrum of 2004 October.

4.2. *Temperature Minimum in the Upper Atmosphere?*

We use a Kurucz model of the photosphere with 6750 K and $\log g = 0.5$ to compute the first-overtone *absorption* band of CO. We adopt a value of 0.5 because it is the smallest gravity model available for this temperature. We perform local thermodynamic equilibrium (LTE) radiative transfer syntheses of the 2.29–2.32 μm wavelength region using Kurucz line lists. The input line data include the 2.3 μm CO band transitions and a number of strong atomic transitions in this NIR region. The top panel of Figure 7 shows the kinetic gas temperature structure of the model. The bottom panel plots the computed spectrum (*dot–long-dashed line*). The computed spectrum only shows some weak atomic absorption lines, without discernible CO features. We checked that noticeable CO absorption can only be computed with models of $T_{eff} \leq 6000$ K, significantly below the values we determine from our spectral monitoring in 2003–2004. These hydrostatic models of the photosphere therefore do not produce strong CO absorption bands in F-type stars such as ρ Cas. The kinetic gas temperatures in the photosphere are too large to yield a sufficient CO abundance, even in the low-gravity conditions of super- and hypergiant atmospheres.

Since we observe that the CO emission variability correlates more strongly with the stellar pulsations than the CO absorption, we model the emission with atmospheric layers in the vicinity of the photosphere. We adapt a Kurucz model for the 2004 September emission spectrum with $T_{eff} = 7250$ K and $\log g = 0.5$ (Fig. 7, *dot–short-dashed line*) by adding a kinetic gas temperature minimum in the upper photospheric layers over a small range of optical depths (*long-dashed, short-dashed*, and *dotted lines*). The modified model produces CO emission when the T_g-minimum is placed below $\log m < -4$ in the column mass scale. The observed emission flux at the CO band head does not appear to be influenced by absorption and can correctly be computed if the T_g-minimum is located around layers with $\log m = -3.1 \pm 0.1$. The latter column mass value corresponds to only $\sim$5% of the mean stellar radius above the photosphere. We apply a projected
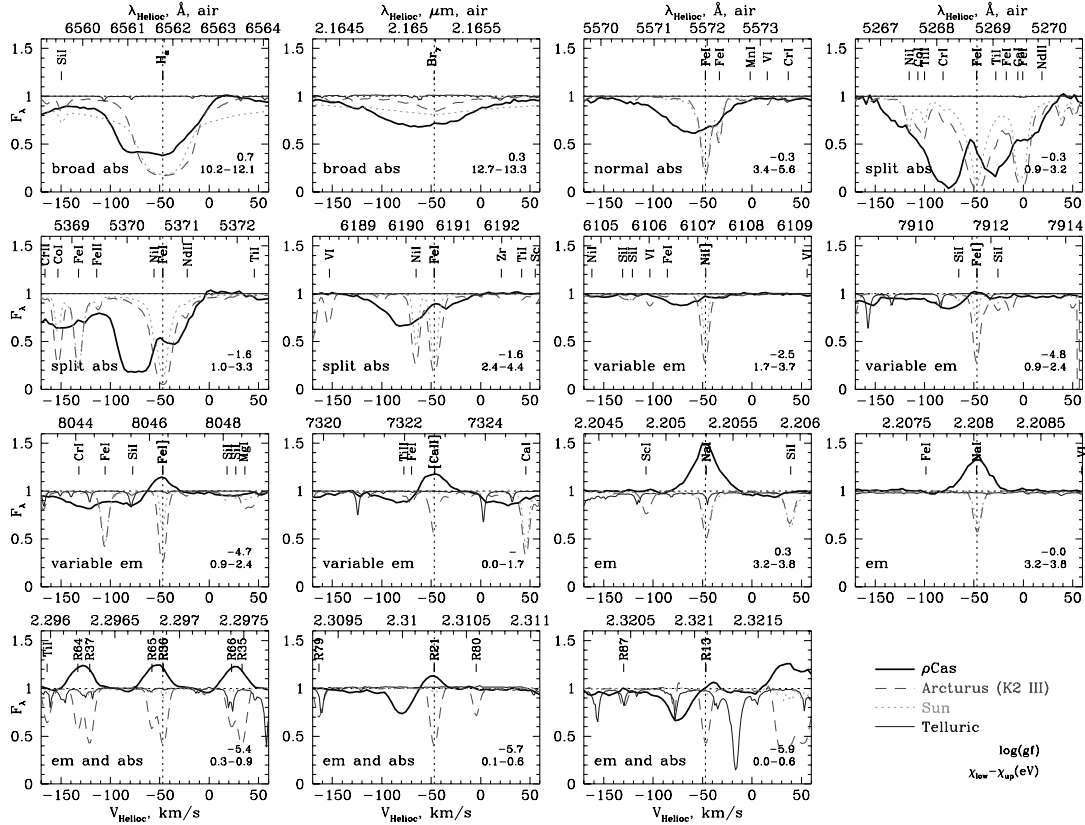
FIG. 8.—Examples of the main types of atomic spectral lines observed in ρ Cas, arranged in progression from pure absorption lines (hydrogen) to pure emission lines (sodium). Compare with the line profiles of several $\Delta\nu = 2-0$ CO transitions. The oscillator strengths and excitation energies of the lower and upper energy levels for a given transition are shown in the bottom right corner. Lines beyond 1 μm are from the CGS4 echelle spectrum of 2004 September, while lines shortward of 1 μm are from the ECHLR spectrum of 2004 October. The spectra of Arcturus, the Sun, and the telluric spectra are from Hinkle et al. (2003). The NIR spectra are corrected for telluric absorption; weak telluric lines remain in the optical. The spectral resolution of all the NIR spectra and of the optical spectrum of ρ Cas is $\sim$40,000, whereas for the optical spectra of the Sun and Arcturus $R \sim 150,000$, which in all cases sufficiently resolves the line profiles for direct comparisons. [*See the electronic edition of the Journal for a color version of this figure.*]

microturbulence velocity broadening of 11 km s^{-1} to compute the NIR spectrum. The supersonic microturbulence velocity fits the observed CO emission-line widths, without invoking extra macroturbulence or rotational line broadening. Our composite model produces the observed CO emission flux. It, however, fails to precisely match the detailed shape of the complete CO band. For example, the computed spectrum obviously lacks sufficient flux longward of the band head. Further improvements of the fit would require an even more detailed atmospheric model with additional modifications in the other thermodynamic conditions besides the T_g-structure (in the current model they are only roughly interpolated to match the extension of the upper temperature profile). More sophisticated and detailed non-LTE radiative transfer calculations of CO would be appropriate in the very low density conditions of our model, but they are beyond the scope of the present investigation.

How can the temperature minimum required in these model fits be produced in the outer atmosphere of ρ Cas? A similar atmospheric temperature structure has been proposed for the Sun to explain the fundamental band of CO at 4.7 μm observed off-limb in emission (Ayres 2002). The solar CO emission forms in the so-called CO-mosphere, a transitional region located between the photosphere and the chromosphere at an altitude of $600-1000$ km. This intermediate emission region is an inhomogeneous gas mixture with an average T_g of $\simeq$3000 K permeated by chromospheric "fingers" of $T_g \sim 10,000$ K. There is, however, no evidence of a classical chromosphere in ρ Cas: the most

important stellar chromospheric indicators such as emission in the cores of the Ca II H and K and Mg II h and k lines have never been observed.

Because we observe the strong NIR CO emission only during variability phases of mean atmospheric expansion, it may indicate an alternative dynamical mechanism that can cause temporal sharp structures in the temperature and density profile of the upper atmosphere. An outwardly propagating field of weak stochastic shock wave trains was, for example, proposed by de Jager et al. (1997) to model the supersonic microturbulence velocities observed in the extended atmosphere of ρ Cas. The CO emission could be produced by a pulsation-driven circumstellar shock wave in the cooling layers behind the shock front where the shocked gas expands while flowing into the following shock wave. After shock passage the cool CO layers are heated by compression in the trailing shock, which partially dissociates the molecular CO gas fraction and quenches its local emission.

5. DISCUSSION

5.1. *Comparing* CO *with Peculiar Atomic Lines*

5.1.1. *Atomic Line Classes*

To compare the NIR CO lines with atomic line profiles, we plot in Figure 8 representative examples for the main line morphology groups observed in ρ Cas. The NIR lines are from the UKIRT spectrum of 2004 September 17 with emission lines during a phase of declining brightness. The optical lines are from the

KPNO spectrum of 2004 October 23 when the emission lines weaken before brightness minimum. Both spectra have comparable spectral resolution of ~ 8 km s^{-1}, sufficient to resolve individual line profiles. Although the emission spectrum weakens in 2004 October (see the CorMASS spectrum in Fig. 4) and the atmospheric expansion must have decelerated somewhat, we believe that the overall line shapes and Doppler shifts do not appreciably change between the two observations (less than $\sim 1/12$ of P apart). We can therefore directly compare the NIR and optical line shapes, within the same pulsation cycle and nearly the same phase, which is crucial for this long-period semiregular variable star.

In Figure 8 we overplot spectral features of ρ Cas with high-resolution spectra of Arcturus (α Boo) and the Sun (both aligned to the rest velocity of ρ Cas), because their spectral lines are narrower and more symmetrical. These reference spectra permit accurate line identifications in ρ Cas whose lines are very broad and often blended or distorted with emission. Furthermore, the effective temperatures of ~ 4400 K (α Boo) and 5800 K (Sun) provide a useful estimate of the sensitivity of the photospheric absorption spectrum with the effective temperature changes of ρ Cas, which can reveal the intrinsic variability of *emission* lines in different pulsation phases. We compare with Arcturus and the Sun despite the larger atmospheric gravity values of $\log g = 1.5$–2.0 (Bell et al. 1985) and 4.4, respectively, than in ρ Cas ($\log g \sim 0$) because detailed synthetic spectra of cool hypergiants are presently not available. Although there is no clear relation between all the spectral lines of these three cool stars (e.g., strong absorption lines in the Sun and Arcturus are sometimes absent in ρ Cas), the comparison reveals that the diverse line profile shapes in ρ Cas are intrinsic to the peculiar spectrum of this hypergiant and do not result from common absorption-line blending.

The optical lines of ρ Cas can be divided into four main groups, which we discuss in more detail as follows.

I. Photospheric absorption lines of neutral and singly ionized metals (e.g., Fe I λ5572 used as the effective temperature indicator in § 4.1). Hydrogen absorption lines can be included in this group as well, although their line formation regions extend far above the photosphere, while Hα can exhibit emission components in both line wings (Fig. 2 of Lobel et al. 2003).

II. "Split" absorption lines with a central emission peak that is essentially constant in both flux and wavelength. In the stronger lines of multiplet [with larger oscillator strengths $\log (gf)$] the wings of the emission core show up against the broad and intensely saturated underlying absorption cores (for example, the Fe I λ5269 line). The cores of weaker lines (such as Fe I λ6191) split only when the absorption core crosses over the central emission peak, which occurs when the radial velocity of the photosphere is similar to its mean. The FWHM of unsaturated split lines is comparable to single absorption lines (~ 60 km s^{-1}) and indicates a common photospheric origin for both.

III. Metallic emission lines of variable strength. They appear prominently above the level of the stellar continuum soon after maximum brightness, but they diminish and then completely vanish around minimum light. A good example of this type of emission line is the semiforbidden Fe I triplet around 0.8 μm.

IV. Metallic emission lines of roughly constant strength. This class includes a few [Ca II] lines and the 2.2 μm Na I emission lines.

Figure 8 shows a number of illustrative lines for each category. They represent a range of line strengths and are minimally blended. The lines progressively change strength from absorption to emission rather than representing separate line groups. The detailed shape of each line appears to depend on the excitation energy, and to a lesser degree on the oscillator strength. Disregarding all hydrogen lines and considering only lines with χ_{low} below a few electron volts, we find that the emission component strengthens while the absorption component weakens with decreasing $\log (gf)$. The Na I 2.2 μm emission lines are the only exceptions because these moderate excitation lines do not show photospheric absorption in F−G stars (Kleinmann & Hall 1986; our Fig. 1).

5.1.2. *Putting CO Lines in the Context*

The NIR CO lines contain both emission and absorption components with very similar profiles compared to the type II and III atomic lines. Note, however, that it has not been established yet if there is any physical difference between the type II and III lines, if they form in two separate atmospheric regions or even with different excitation mechanisms. The morphologic similarity of both line types is apparent with a smooth transformation from emission below the local continuum level in the strongest split lines to (prominent) emission above the continuum for the weaker type III lines (Fig. 8). For example, the central emission cores in the split Na D lines can only rise above the continuum level during the outbursts of ρ Cas (Lobel et al. 2003). Other examples of these mixed line types are presented in Figure 2 of Lobel et al. (2006). Based on the line similarities, Lobel (1997) proposed that emission components in both types emerge from two circumstellar conic shells formed at the interface of a supersonically expanding bipolar wind that collides with previously ejected material from the hypergiant's violent mass-loss history. At the interface the wind velocity decelerates, becomes subsonic, and forms a steady (or standing) shock wave in the outer atmosphere. A curve-of-growth analysis applied to optical multiplets of the central emission cores in split Fe I lines yields an excitation temperature of 3050 K for the shocked region. Provided that these central emission lines are sufficiently optically thin, classical shock wave theory yields a thickness for the bipolar conic shells smaller than or of order the mean stellar radius (using an average mass-loss rate of $\dot{M} = 9 \times 10^{-5}$ $M_{\odot}$ derived from the far-violet extended wings of photospheric absorption lines). The observed emission fluxes yield distances of $15R_* - 150R_*$ from ρ Cas for the location of the emitting shock interface (Lobel 1997, p. 54) for realistic cone opening angles of more than 30°. Smaller opening angles for bipolar outflow would provide distances to the shock interface that exceed estimates in the literature for the distance to the dust formation region near ρ Cas (Jura & Kleinmann 1990).

At these large distances, strong influences of the pulsating photosphere on the emission excitation region are not expected, consistent with the constant flux of the central emission cores of split lines (type II). The Doppler stability of the emission lines with pulsation phase results from the subsonic outflow velocity behind the standing shock wave. We, however, observe different properties for the type III emission lines. These emission lines can appear sporadically in the core of unsaturated absorption lines, and their shapes can alter while the emission varies with the pulsations. It is important to know if these lines are intrinsically variable in total flux and Doppler position. The top panel of Figure 9 shows the time evolution of the unblended emission-free photospheric Fe I λ5572 line during a complete pulsation cycle from 2003 June shortly before minimum light, throughout the maximum of 2004 May, until the minimum of 2005 January. The outburst spectrum of mid-2000 is also shown. The violet line wing develops at the beginning of the brightness decline (the atmospheric expansion can be traced by the blueshifted line centroid) and shrinks back when the star reaches minimum light. The EW (and central depth) of the line increases monotonically
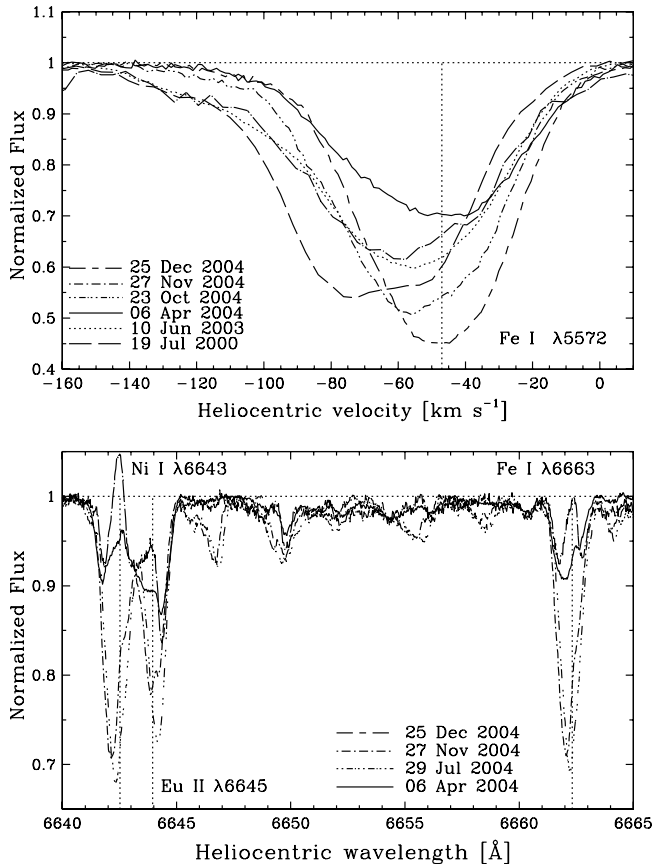
FIG. 9.—High-resolution optical Sofin spectra of ρ Cas during the same pulsation cycle as our NIR CO observations. The top panel shows variations in the high-excitation Fe I $\lambda 5572.84$ absorption line, which probes the variable photospheric radial velocity and changes of effective temperature. The violet line wing forms in the upper atmosphere and probes opacity changes in the supersonic wind of the hypergiant. The core of the neutral iron line remains single throughout the entire pulsation cycle and increases EW when effective temperature decreases. The bottom panel shows three examples of lines that develop emission cores around maximum brightness (type III lines in our terminology). The flux of the emission lines is clearly intrinsically variable, independent of the changes in the underlying photospheric absorption spectrum. [*See the electronic edition of the Journal for a color version of this figure.*]

from maximum to minimum light because the effective temperature decreases. The bottom panel of Figure 9 shows a spectral region with type III lines in the same pulsation cycle. While the absorption spectrum steadily strengthens from 2004 April to December (e.g., the Fe I $\lambda 5572$ and the long-wavelength wing of Eu II $\lambda 6645$ become stronger), the emission component clearly brightens as well between April and July and fades by December. The emission-line evolution resembles the blue wing behavior in the top panel of Figure 9. The variations of the absorption-line wing trace changes of the wind opacity, which also enhances between 2004 April and October. The prominent type III emission lines that peak above the continuum therefore vary intrinsically. Their variability is linked to the photospheric pulsations, since the emission flux increases together with the wind opacity during phases of fast atmospheric expansion.

The detailed evolution of the NIR CO resembles more the type III than the type II lines. The CO emission flux tightly correlates with the pulsations, signaling that it is directly influenced by the photospheric dynamics indicated with our models in § 4. On the other hand, type II emission lines appear invariable and must form farther away from the surface. There are also slight morphological differences between type III/CO and type II emission

lines. The former lines are centered around stellar rest velocity, while the latter are blueshifted by about -5 km s^{-1} due to the subsonic outflow behind the steady shock interface. The type III and the CO emission lines also appear more round-topped compared to the triangular shapes of the strong central emission cores in the optical split lines (Fig. 8). The former lines signal a spherically symmetric line formation region, while the latter lines can emerge from a more conelike outflow observed nearly pole-on. The differences between the two line groups in Doppler shift and line shape are rather subtle, but may be crucial to determine whether or not they belong to two separate emission regions around ρ Cas.

The variability of type III and NIR CO emission lines signals formation regions close to the pulsating photosphere of ρ Cas. But how close? Our model of the CO emission places the formation region at only $\sim$5% of stellar radii because the gas density of the emission region decreases rapidly farther above the surface. Figure 9 reveals, however, that the *optical* emission flux increases together with the wind opacity determined from the far-violet wings of the photospheric absorption lines. The properties of the stellar wind dynamics are determined by the photospheric pulsations and appear to be linked to the emission-line formation region as well. If one could observe a time delay between the increase of the violet absorption-line wings (the mean wind opacity) and the onset of the emission-line spectrum, it would directly provide the distance the wind can travel between the stellar surface [e.g., the base of the stellar wind in the photosphere at $\log (\tau \sim 2/3)$] and the actual emission-line region. A geometric extension of the wind to $\sim 2.5 R_*$ (Lobel et al. 1998) has been modeled from the photospheric absorption lines of ρ Cas, which would disagree with the much smaller distance we determine for the NIR CO. However, part of this difference may arise because our models for the CO band emission assume a LTE approximation that breaks down in the very extended atmosphere and wind of the hypergiant. If, on the other hand, one observes that the emission spectrum develops earlier than the violet wings, then it would favor our shock hypothesis. To discriminate between the two scenarios, a very precise timing of the detailed line profile evolution using more frequent spectroscopic monitoring intervals will be required.

5.1.3. Na I *IR Emission*

We close this section with a discussion of the Na I 2.2 μm doublet lines. These NIR lines are always observed in emission in ρ Cas, even during the deep outburst minimum of 2000–2001 (Fig. 3). The two emission lines of the Na I 2.2 μm doublet are of nearly equal strength. On the other hand, the spectra of nonemission supergiants in Figure 3 show that the short-wavelength absorption line is stronger [due to larger $\log (gf)$ value and blending with other lines] than the longer wavelength one, causing the short-wavelength emission component in the ρ Cas UKIRT outburst spectrum of 2000 October to appear less conspicuous at the medium resolution. The NIR Na I emission is also observed in many other cool Ia and Ia0 supergiants, including HR 8752 (Lambert et al. 1981; McGregor et al. 1988b; Hrivnak et al. 1994; our Fig. 1). It is traditionally explained in the literature to result from pumping by stellar UV radiation, because of the high-excitation energy compared to other optical emission lines. The excitation energy of the upper level is 3.8 eV compared to $\sim$2 eV for optical emission lines. The upper energy level for the Na D core emission can be populated by cascading from the lower level of the NIR Na I doublet through the 1.138 and 1.140 μm transitions. Unfortunately, the latter lines fall in a wavelength region with strong telluric absorption and cannot reliably be

identified in our SpeX spectrum. Calculations of fluorescence were originally carried out for another star: IRC+10420 (Thompson & Boroson 1977). This cool hypergiant has a very large mass-loss rate in quiescence (§ 5.2.1). Thompson & Boroson (1977) considered Mg I lines with relatively high excitation energy ($\chi_{up} = 6$ eV) at 1.5 and 1.7 μm, and concluded based on their strength that they must be optically thick and therefore emerge from a region not far from the photosphere with sufficiently large electron density, such as a stellar chromosphere. There are, however, no clear indications of a classical chromosphere in ρ Cas (§ 4.2). The Mg I lines in the H band of ρ Cas also appear much weaker compared to Na I, unlike in IRC+10420 (e.g., compare the SpeX spectrum in our Fig. 2 with Fig. 7 of Humphreys et al. [2002]). It is therefore not clear if one can postulate the existence of a classical chromosphere in all cool supergiants with the 2.2 μm doublet observed in emission. The rather triangular shapes of the Na I 2.2 μm emission lines can also point to a line formation region in a collimated outflow, rather than in a very extended spherical gas envelope around ρ Cas where the more round-topped forbidden [Ca II] lines form. Independent of the mechanism producing this permanent and strong line emission, the Na I 2.2 μm doublet serves as a powerful indicator for identifying extreme supergiants in the NIR, even from low-resolution spectra.

5.2. Comparing CO Emission and Split Lines in ρ Cas with Other Cool Luminous Stars

The CO absorption lines we observe in ρ Cas can originate in the circumstellar gas envelope, whose existence has been inferred for cooler K−M supergiants from spectral modeling and interferometric NIR measurements (e.g., Tsuji 1988, 2001; Perrin et al. 2004). NIR molecular *emission* bands observed in ρ Cas are, however, a much rarer spectral phenomenon. The emission excitation mechanism is not likely caused by photoionization from a hot companion star because very long-term radial velocity monitoring does not reveal any indication of binarity, while recent far-UV spectroscopy with the *Far Ultraviolet Spectroscopic Explorer* (*FUSE*) confirms that ρ Cas has no significant UV excess either (Lobel et al. 2006), as is, for example, observed for the hot companion in HR 8752 with *IUE*. Variable emission lines in cool stars, however, are often associated with wind variability, bulk movements of circumstellar gas due to wind outflow, or to periodically shocked layers observed in pulsating stars. CO $\Delta\nu$ 2−0 emission lines are observed in low-mass protostars (Biscaya et al. 1997), in hot and cool supergiants (McGregor et al. 1988a; Kraus et al. 2000; Mozurkewich et al. 1987; Matsuura et al. 2002), and in some extreme cases of He-flash objects (such as V838 Mon; Rushton et al. 2005) and novae (Ferland et al. 1979; Rudy et al. 2003). The wind and shock in ρ Cas, however, must be much more optically thin because of the observed absence of emission in the hydrogen lines and of prominent P Cygni−type line profiles (except for Hα).

5.2.1. Cool Hypergiants

How does the NIR spectrum of ρ Cas compare to other luminous cool hypergiants in the upper H-R diagram? The only two objects that at one time have spectroscopically been comparable to ρ Cas are the hypergiants IRC+10420 and HR 8752. IRC+10420 is only ∼0.1 dex more luminous in log (L), while HR 8752 is less luminous by the same amount than ρ Cas (de Jager 1998). Despite the close similarity of the basic stellar parameters, the three hypergiants differ in many other respects. IRC+10420 has a constant mass-loss rate that is an order of magnitude larger than the other two and is also a maser source of the earliest spectral type known. The NIR spectra of 1976 (Thompson & Boroson

1977) and 1984 (Fix & Cobb 1987) revealed Na I emission lines, with the higher members of the Brackett series in absorption, while Brγ was not detected. The weakness of the hydrogen lines at NIR wavelengths was explained with veiling by the spatially resolved dust envelope. In 1992 Oudmaijer et al. (1994) discovered how blueshifted emission features protruded through the NIR hydrogen absorption lines, completely filling them in by 2000 (Humphreys et al. 2002). Interestingly, a weak CO 2.3 μm emission band can be present in the latter spectrum, although it is observed at noise levels. The optical spectra show signs of both out- and downflows. The variability of this cool hypergiant remains poorly studied. Gottlieb & Liller (1978) presented photographic photometry signaling a strongly variable object before 1920 that was steadily increasing in brightness until at least the late 1970s. To reconcile all these observations, Humphreys et al. (2002) suggested that the variable spectrum of IRC+10420 could entirely originate from an opaque circumstellar wind rather than the photosphere, mimicking rapid evolutionary changes in the H-R diagram near the cool boundary of the yellow hypergiant void.

HR 8752 has a less extreme mass-loss rate than IRC+10420, making it more interesting to compare with ρ Cas. It has its own peculiarities, though. The optical and NIR spectra are long-term variable as in IRC+10420. The spectral changes, however, have different properties. The emission spectrum has become systematically weaker, while the absorption spectrum and colors indicate a steady increase in effective temperature of ∼1000 K per decade over the past 30 years. The photospheric pulsations have almost ceased, while the V amplitude decreased from ±0.2 mag in the early 1980s, to ±0.05 mag in the mid-1990s (Percy & Zsoldos 1992; Nieuwenhuijzen & de Jager 2000). From 1960 until 1980 it was in all aspects very similar to ρ Cas, including periodic line doubling and the occurrence of emission lines (interestingly also in NIR CO), with both emission and absorption components that altered with the pulsation phase (Harmer et al. 1978; Lambert & Luck 1978; Lambert et al. 1981; Sheffer & Lambert 1987; Sheffer 1993).

We compare the NIR CO spectra of HR 8752 from Sheffer (1993) with the brightness curve and observe that the CO emission lines appear at the stellar rest velocity while the emission flux peaks around maximum brightness, as we also observe in ρ Cas. The CO absorption varies less regularly and may occur both red- and blueshifted. Surprisingly, by 1988 the NIR CO band disappears completely, followed by type II and a flux decline in the type III emission lines. The absorption lines remain, however, very broad, as observed in the optical spectrum of HR 8752 in 1998 by Israelian et al. (1999). We observe no trace of NIR CO in our CorMASS spectra of 2003 November and 2004 October (Fig. 1). The Na I 2.2 μm emission lines are still observed, although Sheffer (1993) reported a decrease of the line fluxes. Unlike ρ Cas, HR 8752 has a main-sequence early B-type companion that may contribute to the hypergiant's emission spectrum. For example, the [N II] $\lambda\lambda$6548, 6583 lines are thought to originate in a Strömgren sphere surrounding the companion, but we do not observe them in ρ Cas. What caused the disappearance of CO and other low-excitation lines observed before 1987 in HR 8752? We suggest that either the decrease of the photospheric pulsation amplitude weakened the shock wave(s) that can excite these emission lines, or that CO molecules close to the photosphere dissociated with the large increase of effective temperature during subsequent decades. But what can cause this very fast increase of effective temperature? Possibly we observe this hypergiant in transit across the yellow evolutionary void, on its way of becoming a blue supergiant. Or perhaps its atmosphere is warming up

with the approach of the hot companion. Another possible explanation is that HR 8752 exhibits long-term secular variability, perhaps comparable to the changes from more to less regular atmospheric oscillations that we also observe for ρ Cas. Continued spectroscopic and photometric monitoring of these unique luminous cool objects is needed to address these questions in further detail.

5.2.2. Post-AGB Supergiants

Hypergiants are very exceptional luminous stars. Further insights into their NIR spectroscopic variability can be gleaned from more abundant and more regularly pulsating less luminous cool supergiants. Good examples of stars for which we also observe NIR CO in emission are a number of yellow post-AGB stars and some proto−planetary nebulae precursors. It is unclear at present whether NIR CO emission occurs more frequently in variable stars or for a certain spectral type or subclass. Hrivnak et al. (1994) found three proto−planetary nebular supergiants with CO emission. The earliest is G0 Ia IRAS 22223+4327, a pulsating variable. McGregor et al. (1988b) found CO emission in a few early-type Ia supergiants in the Magellanic Clouds, but they are not known to be photometrically variable. The earliest reported case is the RV Tau F4−type Ibp star AC Her (HD 170756), which also shows Brγ in absorption and Na I 2.2 μm in emission similar to ρ Cas. NIR CO in this star switched from emission to absorption in three low-resolution spectra of Oudmaijer et al. (1995). We have reduced an archival CGS4 spectrum of another post-AGB Srd variable star with NIR CO emission: HD 179821 (G5 Ia). The spectrum was obtained on the same night of 2000 October 18 as the outburst spectrum of ρ Cas. It shows the Na I 2.2 μm lines in emission but not a trace of CO, confirming the CO variability previously noted by Oudmaijer et al. (1995).

5.2.3. R CrB Stars and ρ Cas Outbursts

The NIR CO bands observed in R CrB stars offer an interesting comparison to ρ Cas. These less luminous eruptive variables have carbon-rich and hydrogen-deficient atmospheres, but exhibit many similarities to ρ Cas otherwise. They cover the same range of effective temperature, reveal prominent emission lines at times, and are known pulsators that most importantly exhibit deep visual brightness declines (Clayton 1996). It is thought that occultations by dense dusty circumstellar clouds cause the abrupt dimming. The dust clouds should occur rather close to the photosphere, dictated by the short timescales of the sudden brightness decreases. But how can dust form at photospheric gas temperatures above 5000 K in these F−G type stars? Hinkle et al. (1995) observed the CO 2.3 μm band in FG Sge, a post-AGB and He-flash supergiant, 2 months before it went into a deep brightness decline, which turned it into a typical R CrB star thereafter. They observed split CO line profiles with one absorption component near the stellar rest velocity and the other blueshifted by 21 km s^{-1}. The CO lines are interpreted as evidence of a long-sought reservoir of cool material forming near the stellar surface. After the first circumstellar gas shell forms at a distance of $\sim 2R_*$, the second shell cools below 1000 K and forms dust while becoming accelerated outward by radiation pressure on the dust. Based on these observations, Gonzalez et al. (1998) proposed that CO gas might be the leading coolant initiating the nucleation of dust grains very close to the photosphere. However, a very recent extended study of R CrB stars by Tenenbaum et al. (2005) did not establish any clear correlation between the appearance of the 2.3 μm CO band and phases of large brightness decrease. In fact, they modeled the observed CO band strengths with pure

photospheric models. Their work points to a strong connection with ρ Cas for which we observe that the absorption-line splitting is due to a pulsation phase-dependent superposition of absorption and emission-line components that recur on a regular basis, rather than being direct tracers of cool circumstellar material expelled during outbursts.

There are convincing indications that the trigger for dust formation is actually located in the photosphere of R CrB stars. Gonzalez et al. (1998) found that the photosphere cools by at least ~ 1000 K during the fast brightness declines. This atmospheric phenomenon is often neglected because of difficulties in interpreting R CrB spectra observed at brightness minima. The absorption lines appear to weaken and to become distorted, possibly because the photospheric spectrum is blurred by the scattering from the expanding dust clouds (although these effects are not clearly observed in ρ Cas). The atmospheric cooling itself appears to result from some kind of dynamic transformation or instability. Kameswara Rao et al. (1999; see their Fig. 1) observed that at the beginning of a strong brightness decrease in R CrB, the low-excitation photospheric lines reveal an emission component and become strongly redshifted. The high-excitation lines, in contrast, become blueshifted. This signals that the upper atmosphere decouples from the regular pulsation movements. The photosphere collapses, causing a stronger than usual compression, which in turn results in a stronger than usual atmospheric expansion with a large brightness decrease. A very similar behavior is observed during the 2000−2001 outburst of ρ Cas. The event was preceded by a strong collapse of the atmosphere that reversed to expansion and subsequently cooled the entire atmosphere down by more than 3000 K. The larger brightness decreases in R CrB stars compared to the outbursts of ρ Cas are likely due to more vigorous dust formation around the former stars. The enhanced dust formation may be caused by the large carbon abundance and hydrogen deficiency of R CrB atmospheres. Whether or not there is dust formation during the outbursts of ρ Cas, it appears reasonable to attribute the sudden eruptions to a common physical mechanism operating in the atmospheres of cool hypergiants and R CrB stars. Lobel et al. (2003) showed that the recombination of partially ionized hydrogen in ρ Cas, and the recombination of ionized helium in R CrB stars, can effectively drive a runaway explosion over the timescales corresponding to the observed brightness declines of both eruptive variables. The eruptions are triggered by unusual thermal conditions in F-type stars during phases of very strong atmospheric compression causing a dynamically unstable atmosphere (Lobel 2001). Lobel et al. (2003) proposed that the stellar wind and oscillations can suddenly activate the trigger, which we observe is tightly correlated with the occurrence of strong emission-line spectra. The study of strong transient emission lines in different types of luminous pulsating cool stars therefore provides important clues to the physical mechanisms that produce the large diversity of their observed light curves.

R CrB stars both in and out of the sudden brightness declines reveal many spectral similarities with ρ Cas. Most noticeably, the photospheric lines of R CrB stars are very broad as in F-type hypergiants (Pandey et al. 2004). The lines sometimes split around phases of maximum brightness, which appears to correlate with the radial velocity amplitude. In RY Sgr, having a pulsation amplitude of ± 20 km s^{-1}, the split lines occur regularly, while in R CrB, having an amplitude of only ± 3 km s^{-1}, they are not observed every pulsation cycle, except in the strongest lines (Kameswara Rao & Lambert 1997); ρ Cas has an intermediate velocity amplitude of ± 8 km s^{-1}, between these two values. The brightness declines are preceded by an increase of the pulsation

amplitude, observed, for example, in R CrB (Kameswara Rao et al. 1999), and in ρ Cas by Lobel et al. (2003). Possibly, it is therefore no surprise that the emission-line spectrum also strengthens during variability phases preceding the outbursts of R CrB stars. The so-called E1 group in R CrB stars represents transient sharp emission lines that are only briefly observed at the very onset of the declines. The E1 group may therefore correspond to our variable type III emission lines in ρ Cas. On the other hand, the so-called E2 group of emission lines has spectral characteristics identical to our type II lines. These emission lines are sharp cores inside low-excitation absorption lines and are permanently blueshifted by $3-5$ km s^{-1} relative to the star velocity. They are apparently of constant flux and appear most prominently in the middle of the fast brightness declines when the stellar continuum flux significantly decreases (Cottrell & Lambert 1982; Gonzalez et al. 1998; Kameswara Rao et al. 1999; Skuljan & Cottrell 2002). Sharp emission-line components above the local continuum level are observed during brightness minimum in R CrB stars in forbidden lines such as [Ca II] and in resonance doublet lines of K I (0.77 μm) and Na D (0.59 μm). The narrow emission components, however, do not occur in Mg II h and k lines (at 0.28 μm) or Ca II H and K lines (0.39 μm) (Clayton et al. 1994; Kameswara Rao et al. 1999), which again compares to the observations of ρ Cas. NIR Na I or CO emission lines have never been reported in R CrB stars, possibly because this spectral region has not been thoroughly investigated. The optical C$_2$ bands, however, are observed to appear in emission at the onset of the brightness declines. They either remain in emission or return to absorption around minimum brightness, although a clear correlation with the pulsation phase or phases of brightness declines has yet to be established (Gonzalez et al. 1998; Kameswara Rao et al. 1999; Skuljan & Cottrell 2002). The two most significant spectroscopic *differences* between R CrB stars and ρ Cas are the presence in the spectrum of the former and the absence in the latter of (1) a strong He I 1.083 μm line with a P Cygni profile (although with notable exceptions for warmer $T_{\rm eff} > 6000$ K stars as V854 Cen), indicative of warm chromospheric winds in R CrB stars (Clayton et al. 2003); and (2) a broad (FWHM > 200 km s^{-1}) emission component observed during R CrB brightness declines in forbidden and permitted strong lines (such as Hα, He, and metal resonance lines), which Kameswara Rao et al. (1999) suggested can result from an accretion disk around a putative white dwarf companion star (but note that a hot companion is not observed in ρ Cas).

5.2.4. *Line Splitting and Pulsations*

There is ample evidence from the literature that other long-period cool variables such as Cepheids, RV Tau stars, R CrB stars, and Miras show absorption-line splitting and emission lines above the continuum level around phases of maximum brightness, in atomic as well as molecular lines of CO and CN (Sanford 1952; Kovtyukh et al. 2003; Alvarez et al. 2001; Mozurkewich et al. 1987; Kameswara Rao & Lambert 1997; Nowotny et al. 2005b). The line-splitting phenomenon is also observed in hot RR Lyr variables (Chadid & Gillet 1996). Based on the above discussion, we think it is merely a matter of coordinating coeval optical and NIR observations to firmly establish that phase-dependent spectral changes in absorption-line splitting and emission-line flux are related spectroscopic phenomena, because spectral variability is clearly linked with changes of effective temperature in cool pulsating stars. These spectral phenomena are widespread among pulsating stars of various types in the cool part of the H-R diagram. They should therefore be attributed to radiative transfer effects that result from atmospheric pulsations instead of expanding circumstellar gas shells that are simply postulated by default for detailed calculations of mass-loss rates.

5.3. *Emission by the Running Shock Wave?*

Considerable theoretical work has been published to model emission lines in *cool* pulsating stars. Among all cool stars with split absorption lines, the Mira variables are possibly best studied with recent dynamic models of the atmosphere that quite well match the observed line profiles. In most studies, however, the apparent absorption components of split absorption lines are still interpreted to result from separate detached layers (optically thick shells) with different Doppler velocities. The double line cores are simply assumed to have a purely kinematic origin (Bessel et al. 1996; Winters et al. 2000; Nowotny et al. 2005a, 2005b). The alternative interpretation we propose with a central emission reversal inside the absorption-line core is computationally much more challenging and has only very recently been explored with radiative transfer calculations. Richter et al. (2003) considered specific spectroscopic examples with Fe II and [Fe II] emission lines that occur in some Miras only after exceptionally large brightness maxima (or equivalently very strong atmospheric compression). They demonstrated that these emission lines can be excited in a confined postshock layer close to the stellar photosphere at $1R_* - 2R_*$. The postshock gas is heated by the passage of a shock wave produced in the photosphere, which reaches this emission layer in half a pulsation cycle. For the shock to be sufficiently strong to produce emission lines, a minimum shock velocity of ~ 20 km s^{-1} is required in Miras. In an earlier study, Woitke et al. (1996) already demonstrated that adiabatic cooling of shocked gas can yield sufficiently small gas temperatures for the nucleation of dust grains within the same close distance of $1.5R_* - 3R_*$ from the photosphere of R CrB stars. The local gas density and shock velocity are the prime factors that determine the location of the emission zone. These models support the small distances of only $\lesssim 1R_*$ that we compute for the NIR CO emission-line formation region in ρ Cas with a simplified atmosphere model in which the outer gas temperature structure is modified by a shock wave.

Some difficulties, however, remain when trying to directly apply the above models to the warm yellow hypergiants ρ Cas and HR 8752. It should be remembered that radiation pressure on dust around the dust condensation radius (at a few stellar radii) is considered to be the driving mechanism of winds and mass loss in all modern models of R CrB and Mira variables. In ρ Cas, however, there is no evidence so far of significant dust nucleation close to the photosphere. The weak 9.8 μm silicate dust emission feature and the IR spectral energy distribution place the dust envelope (possibly resulting from the outburst of $1945-1946$) at $30R_* - 130R_*$ from the star (Jura & Kleinmann 1990). New IR photometry and spectroscopy after the $2000-2001$ outburst would help to further determine the properties of circumstellar dust in ρ Cas.

Furthermore, some constraints from our NIR CO emission models can be used to estimate the velocity of the shock wave near ρ Cas. When index 1 denotes the preshock (upstream) gas conditions T_1, p_1, and ρ_1, and index 2 denotes the postshock (downstream) conditions (with jump conditions across a compression shock surface: $T_2 > T_1$, $p_2 > p_1$, and $\rho_2 > \rho_1$), the speed of the shock u_1 can be expressed through the local adiabatic speed of sound and the Mach number: $u_1 = c_1 M_1$. For a specific heat ratio of ideal monatomic gas of $\gamma = 5/3$ (assuming hydrogen gas) to 7/5 (for CO gas with rotational degrees of freedom) and the mean gas pressure and density structures of our atmosphere model (§ 4.2), we compute $c_1 = (\gamma p_1/\rho_1)^{1/2} = 7.5-7$ km s^{-1}. The preshock Mach number M_1 can be computed

with the classical Rankine-Hugoniot jump relations in polytropic gas, which are a function of γ and T_2/T_1 only. For $T_2/T_1 = 4200/2500$ K (Fig. 7) we compute $M_1 = 1.30$–1.36. We thus obtain a shock velocity of $u_1 \sim 10$ km s^{-1}. This value is smaller than the 20 km s^{-1} threshold velocity required in the shock models to excite atomic emission lines, and yet they are observed in every pulsation cycle in ρ Cas; 10 km s^{-1} is in fact only a lower limit, since T_2 (the gas temperature of the postshock region) can be much larger than the 4200 K we adopt from the unperturbed model atmosphere. On the other hand, the nondetection of dust formation in the vicinity of the photosphere of ρ Cas appears consistent with the small velocity (or Mach number) of the shock wave(s).

Alvarez et al. (2001) conducted a large survey of the absorption-line doubling phenomenon in long-period variables. They demonstrate that it is more frequently observed among stars with compact rather than extended atmospheres and interpret it to result from stronger shock waves in the former stars. Hypergiants such as ρ Cas and HR 8752 with their enormous stellar radii of several hundreds of solar radii clearly do not follow this trend. On the contrary, HR 8752 has become more compact as the effective temperature has dramatically increased over the past 30 years, but the split absorption lines are presently no longer observed in its optical spectrum compared to the 1970s. If the line broadening of these split lines were solely due to a superposition of two absorption components emerging from two separate gas layers above and below the shock surface, predicted with models of Miras, the width of these lines would have to decrease with the disappearance of the shock waves in the atmosphere of HR 8752. This is, however, not observed because the photospheric lines typical of a hypergiant spectrum have remained very broad.

Our model for the central emission excited by a propagating shock wave possesses some difficulties as well. A shock wave propagating supersonically in the stellar rest frame should produce redshifted CO line emission (provided the emission is sufficiently optically thick), which we do not observe. Another problem is that a transient and spatially rather narrow atmospheric structure required for the CO emission cannot readily account for the permanent excitation of other static (and apparently centered around stellar rest) atomic emission lines in our high-resolution spectra.

In summary, none of the available theoretical models of the atmospheric dynamics can coherently explain the absorption-line splitting and line emission phenomenon in pulsating cool supergiants. The field of research is making rapid progress, however. The current investigation shows that the correct answer may be obtained with the development of a new generation of atmospheric models that couple the dynamics of the atmosphere with non-LTE excitation of spectral lines in shock waves.

6. SUMMARY AND CONCLUSIONS

We describe a high-resolution spectroscopic study of one of the most luminous cool stars in the Galaxy, the bright yellow hypergiant ρ Cas. Our observations cover a complete pulsation cycle in 2003–2004 over a large wavelength range from the optical to ~ 4 μm. NIR spectroscopic studies of yellow supergiants are scarce, and we demonstrate that the emission lines they harbor serve as powerful diagnostics of the important atmospheric processes of mass loss and pulsation in massive stars. In particular, we identify several prominent emission lines in the L-band spectrum observed near maximum brightness and present K-band spectra obtained during the last grand outburst of the enigmatic hypergiant in 2000–2001.

We primarily investigate the first-overtone band of CO at 2.3 μm because it occurs prominently in emission during certain variability phases of ρ Cas. The NIR CO band is believed to originate from expanding shells and to trigger the formation of dust close to the photosphere of R CrB stars. We confirm the findings of Sheffer (1993) that the CO band in ρ Cas is variable and consists of absorption- and emission-line components. However, based on detailed comparisons with atomic lines and correlating all spectroscopic observations with the corresponding pulsation phases, we argue that the split absorption-line profiles are not caused by two separately ejected shells during rare outbursts of the hypergiant, but rather are a commonly observed combination of a static narrow central emission line superimposed on the core of a broad absorption line. The absorption line exhibits Doppler displacements due to the atmospheric pulsations, while the emission component is always centered around the stellar rest velocity. The flux of the central emission line varies with the pulsations of the photosphere and rises above the continuum level around maximum brightness during phases of fast atmospheric expansion. After the phase of minimum brightness, the emission flux decreases and the lines fade. Detailed comparisons of NIR CO line profiles with low-excitation atomic lines reveal that they are intermediate between the type II and type III lines of ρ Cas (according to our terminology). While CO absorption components are always present and vary similarly to permanently split atomic absorption lines (type II), the large variability of the superimposed CO emission components suggests they are more compatible with the type III emission lines that can appear above the level of the stellar continuum flux. In other words, the excitation mechanism of prominent atomic emission lines and CO emission we observe in ρ Cas can have a common physical origin.

The strong correlation of the NIR CO emission flux we observe with the radial velocity curve from photospheric pulsations signals that the CO emission lines form in the vicinity of the photosphere. We model the CO emission band spectra by inserting a cool gas layer of $T_g \sim 2500$ K in the kinetic gas temperature structure of a plane-parallel hydrostatic Kurucz model of the photosphere with $T_{\rm eff} = 7250$ K and $\log g = 0.5$. We fit the observed emission flux around the CO band head, which is least influenced by absorption, with radiative transfer calculations to constrain the optical depth of the cool CO layer. We determine an atmospheric column mass along the line of sight of $10^{-3.1\pm0.1}$ g cm^{-2}. It translates to a geometric distance for the cool CO layer of only $\sim 5\%$ of stellar radii above the photosphere.

We further compare the evolution of NIR emission lines in ρ Cas with the spectra of other late-type supergiants. We consider cool Miras, the yellow hypergiants HR 8752 and IRC+10420, some less luminous post-AGB stars, and their Population II analogs of R CrB stars with large visual brightness declines. We observe a number of important spectroscopic similarities between all these cool variable star types. The most remarkable are as follows: (1) when several epochs of observations are available, the NIR CO emission flux is always observed to vary; (2) the CO emission flux is largest around maximum brightness, also observed in prominent atomic emission lines; (3) prominent emission lines and split absorption lines are more frequently observed in stars with larger pulsation amplitudes or with larger radial velocity amplitudes; (4) the onset of (sudden) strong brightness decreases in ρ Cas and R CrB stars results from a stronger than usual compression of the photosphere followed by a stronger than usual expansion and cooling of the entire atmosphere with the appearance of the type III variable emission lines we propose are analogous to type E1 emission lines observed in R CrB stars; and (5) during the fast brightness declines of outbursts, the initial emission-line spectrum is replaced by another type of emission line, the so-called E2 lines in R CrB stars, and in ρ Cas the type II

emission-line cores of split absorption lines. We propose that the latter types of emission lines are always present but become more obvious during fast brightness declines because the mean photospheric flux suddenly decreases.

In summary, we identify two groups of narrow emission lines with FWHM < 50 km s^{-1} that coexist in the spectra of low-gravity pulsating stars. The first group consists of atomic lines that appear to be intrinsically invariable (types II and IV in our terminology). The second group consists of atomic and CO emission lines that are intrinsically variable (type III). Both groups are low-excitation lines with χ_{low} of order a few electron volts having Doppler velocities of ~5 km s^{-1} around the stellar rest velocity. The excitation of both groups appears to be related in one way or another to the atmospheric pulsations. The best interpretation we can propose based on our NIR spectroscopic observations is that the second group is excited in a short-lived circumstellar cool gas layer in the immediate vicinity of the photosphere less than $1R_*$ away that is excited by the passage of a pulsation-driven shock wave. The first group of emission lines is excited in two static conic regions $\sim10R_*-100R_*$ above the photosphere (Lobel et al. 2003), where the supersonic wind of ρ Cas collides with circumstellar material (and possibly replenished by recurrent outbursts) forming a permanently standing shock wave.

The following list of observations would be helpful to further verify our interpretations:

1. Very high resolution spectroscopic observations ($R \gtrsim 100,000$) of type II and III emission lines in ρ Cas to search for possible differences in radial velocity and line profile shapes between both groups. The observations could confirm if the emission lines form in two spatially separate regions in the circumstellar environment of the hypergiant.

2. High-resolution spectroscopic observations beyond 3 μm to identify and investigate the properties of other prominent emission lines expected in this wavelength region.

3. Monitoring of the *fundamental* band of CO at 4.6 μm to determine how far out the photospheric pulsations and shock waves propagate into the circumstellar environment.

4. New observations of the silicate 9.8 μm dust emission feature after the outburst of 2000–2001. NIR and far-IR photometry can establish if ρ Cas produces dust during the large brightness decreases of outbursts. It can further link its remarkable atmospheric dynamics to that of other eruptive variable stars.

5. High-resolution spectroscopic monitoring of NIR CO and split absorption lines in other late-type stars. In particular, observations of semiregular pulsating variables (e.g., RV Tau, and R CrB stars) can test the relative importance of the pulsations versus effective temperature for sustaining the cool gas layers that produce the peculiar emission-line spectra.

APPENDIX

SPECTRAL LINE IDENTIFICATION LISTS

Table 3 provides wavelengths of spectral lines marked in the figures of this paper. Sources of wavelengths we used are as follows.

1. Atomic Line List, version 2.04, compiled by P. van Hoof.[7]
2. 1995 Atomic Line Data by R. L. Kurucz & B. Bell.[8]
3. CO Line List by R. L. Kurucz.[9]

[7] See http://www.pa.uky.edu/~peter/atomic.
[8] See http://cfa-www.harvard.edu/amdata/ampdata/kurucz23/sekur.html.
[9] See http://kurucz.harvard.edu/LINELISTS/linesmol/coxx.asc.

TABLE 3
LIST OF OBSERVED SPECTRAL LINES

λ^{a} (Å)	Element	Figure Number
5572.842	Fe I	8, 9
5269.537	Fe I	8
5371.489	Fe I	8
6191.557	Fe I	8
6108.116	Ni I]	8
6562.80	Hα	1, 8
6643.630	Ni I]	9
6645.064	Eu II	9
6663.441	Fe I	9
7323.89	[Ca II]	8
7771.944, 7774.166, 7775.387	O I	1
7912.866	Fe I]	8

TABLE 3—*Continued*

λ^{a} (Å)	Element	Figure Number
8047.617	Fe I]	8
8203.6	Pa$_{lim}$	1
8498.03, 8542.09, 8662.14	Ca II	1
9229.014	Paζ	1
10036.653	Sr II	1
10049.373	Paδ	1
10114.015	Fe I	1
10123.86	C I	1
10124.940	Si I	1
10327.311	Sr II	1
10396.76	Ti I	2
10455.449, 10456.757, 10459.406	S I	1
10683.08, 10685.34, 10691.24	C I	1
10914.887	Sr II	1
10938.095	Paγ	1
12818.08	Paβ	1
14584.2	Br$_{lim}$	1
15024.993	Mg I	2
15700.662	Br$_{15}$	1
15880.541	Br$_{14}$	1, 6
16109.313	Br$_{13}$	1, 6
16407.192	Br$_{12}$	1, 6
16806.520	Br$_{11}$	1, 6
17108.663	Mg I	2
17362.108	Br$_{10}$	1, 6
20629.757	Fe I	3
21163.76	Al I	3
21354.226	Si I	3
21655.29	Brγ	1, 3, 4, 5, 6, 8
21782.7	Ti I	3
21874.15	Si I	3
21897.3	Ti I	3
22004.3	Ti I	3
22024.3	Sc I]	3
22056.4	Na I	1, 2, 3, 4, 5, 6, 8
22083.7	Na I	1, 2, 3, 4, 5, 6, 8
22210.6	Ti I	3
22232.9	Ti I	3
22257.108	Fe I	3
22266.7	Sc I	3
22274.0	Ti I	3
22624.97, 22626.73	Ca I	3
22651.18, 22653.58, 22655.35	Ca I	3
22928.976	^{12}CO $\Delta\nu$ 2−0 band head	1, 2, 3, 4, 5, 6, 7
22972.326	ΔJ 36−37	5, 8
23106.100	ΔJ 21−22	5, 8
23214.513	ΔJ 13−14	5, 8
23220.222	^{12}CO $\Delta\nu$ 3−1 band head	2
23518.163	^{12}CO $\Delta\nu$ 4−2 band head	2
23822.970	^{12}CO $\Delta\nu$ 5−3 band head	2

[a] Rest wavelength in air.

REFERENCES

Alvarez, R., Jorissen, A., Plez, B., Gillet, D., Fokin, A., & Dedecker, M. 2001, A&A, 379, 305
Arellano Ferro, A. 1985, MNRAS, 216, 571
Ayres, T. R. 2002, ApJ, 575, 1104
Banerjee, D. P. K., & Ashok, N. M. 2002, A&A, 395, 161
Bell, R. A., Edvardsson, B., & Gustafsson, B. 1985, MNRAS, 212, 497
Bessel, M. S., Scholz, M., & Wood, P. R. 1996, A&A, 307, 481
Bidelman, W. P., & McKellar, A. 1957, PASP, 69, 31
Bieging, J. H., Rieke, M. J., & Rieke, G. H. 2002, A&A, 384, 965
Biscaya, A. M., Rieke, G. H., Narayanan, G., Luhman, K. L., & Young, E. T. 1997, ApJ, 491, 359
Chadid, M., & Gillet, D. 1996, A&A, 308, 481

Clayton, G. C. 1996, PASP, 108, 225
Clayton, G. C., Geballe, T. R., & Bianchi, L. 2003, ApJ, 595, 412
Clayton, G. C., Lawson, W. A., Cottrell, P. L., Whitney, B. A., Stanford, S. A., & de Ruyter, F. 1994, ApJ, 432, 785
Cottrell, P. L., & Lambert, D. L. 1982, Observatory, 102, 149
Cushing, M. C., Vacca, W. D., & Rayner, J. T. 2004, PASP, 116, 362
de Jager, C. 1998, A&A Rev., 8, 145
de Jager, C., Lobel, A., & Israelian, G. 1997, A&A, 325, 714
Ferland, G. J., Lambert, D. L., Netzer, H., Hall, D. N. B., & Ridgway, S. T. 1979, ApJ, 227, 489
Fix, J. D., & Cobb, M. L. 1987, ApJ, 312, 290
Gesicki, K. 1992, A&A, 254, 280

Gillet, D., Duquennoy, A., Bouchet, P., & Gouiffes, C. 1989, A&A, 215, 316

Gonzalez, G., Lambert, D. L., Wallerstein, G., Rao, N. K., Smith, V. V., & McCarthy, J. K. 1998, ApJS, 114, 133

Gottlieb, E. W., & Liller, W. 1978, ApJ, 225, 488

Harmer, D. L., Lawson, P. A., & Stickland, D. J. 1978, Observatory, 98, 250

Hauschildt, P. H., Allard, F., Ferguson, J., Baron, E., & Alexander, D. R. 1999, ApJ, 525, 871

Hinkle, K. H., Hall, D. N. B., & Ridgway, S. T. 1982, ApJ, 252, 697

Hinkle, K. H., Joyce, R. R., & Smith, V. 1995, AJ, 109, 808

Hinkle, K., Wallace, L., Livingston, W., Ayres, T., Harmer, D., & Valenti, J. 2003, in Cool Stars, Stellar Systems, and the Sun, ed. A. Brown, G. M. Harper, & T. R. Ayres (Cambridge: Cambridge Univ. Press), 851, http://www.archive.noao.edu, ftp://ftp.noao.edu/catalogs/hiresK

Hrivnak, B. J., Kwok, S., & Geballe, T. R. 1994, ApJ, 420, 783

Humphreys, R. M. 1978, ApJS, 38, 309

Humphreys, R. M., Davidson, K., & Smith, N. 2002, AJ, 124, 1026

Ilyin, I. 2000, Ph.D. thesis, Univ. Oulu

Israelian, G., Lobel, A., & Schmidt, M. R. 1999, ApJ, 523, L145

Jura, M., & Kleinmann, S. G. 1990, ApJ, 351, 583

Kameswara Rao, N., & Lambert, D. L. 1997, MNRAS, 284, 489

Kameswara Rao, N., et al. 1999, MNRAS, 310, 717

Kleinmann, S. G., & Hall, D. N. B. 1986, ApJS, 62, 501

Kovtyukh, V. V., Andrievsky, S. M., Luck, R. E., & Gorlova, N. I. 2003, A&A, 401, 661

Kovtyukh, V. V., & Gorlova, N. I. 2000, A&A, 358, 587

Kraus, M., Kraegel, E., Thum, C., & Geballe, T. R. 2000, A&A, 362, 158

Lambert, D. L., Hinkle, K. H., & Hall, D. N. B. 1981, ApJ, 248, 638

Lambert, D. L., & Luck, R. E. 1978, MNRAS, 184, 405

Lejeune, T., & Schaerer, D. 2001, A&A, 366, 538

Lobel, A. 1997, Pulsation and Atmospherical Instability of Luminous F- and G-Type Stars: The Yellow Hypergiant ρ Cassiopeiae (Maastricht: Shaker)

———. 2001, ApJ, 558, 780

———. 2004, Mercury, 33, 13

Lobel, A., Aufdenberg, J., Ilyin, I., & Rosenbush, A. E. 2006, in Cool Stars, Stellar Systems, and the Sun, ed. F. Favata et al. (ESA-SP 560; Noordwijk: ESA) (astro-ph/0504524), in press

Lobel, A., de Jager, C., Nieuwenhuijzen, H., Smolinski, J., & Gesicki, K. 1994, A&A, 291, 226

Lobel, A., Israelian, G., de Jager, C., Musaev, F., Parker, J. W., & Mavrogiorgou, A. 1998, A&A, 330, 659

Lobel, A., et al. 2003, ApJ, 583, 923

Lynch, D. K., et al. 2004, ApJ, 607, 460

Matsuura, M., Yamamura, I., Zijlstra, A. A., & Bedding, T. R. 2002, A&A, 387, 1022

McGovern, M. R., Kirkpatrick, J. D., McLean, I. S., Burgasser, A. J., Prato, L., & Lowrance, P. J. 2004, ApJ, 600, 1020

McGregor, P. J., Hyland, A. R., & Hillier, D. J. 1988a, ApJ, 324, 1071

———. 1988b, ApJ, 334, 639

Mountain, C. M., Robertson, D. J., Lee, T. J., & Wade, R. 1990, Proc. SPIE, 1235, 25

Mozurkewich, D., Gehrz, R. D., Hinkle, K. H., & Lambert, D. L. 1987, ApJ, 314, 242

Nieuwenhuijzen, H., & de Jager, C. 1995, A&A, 302, 811

———. 2000, A&A, 353, 163

Nowotny, W., Aringer, B., Höfner, S., Gautschy-Loidl, R., & Windsteig, W. 2005a, A&A, 437, 273

Nowotny, W., Lebzelter, T., Hron, J., & Höfner, S. 2005b, A&A, 437, 285

Oudmaijer, R. D., Geballe, T. R., Waters, L. B. F. M., & Sahu, K. C. 1994, A&A, 281, L33

Oudmaijer, R. D., Waters, L. B. F. M., van der Veen, W. E. C. J., & Geballe, T. R. 1995, A&A, 299, 69

Pandey, G., Lambert, D. L., Rao, N. K., Gustafsson, B., Ryde, N., & Yong, D. 2004, MNRAS, 353, 143

Percy, J. R., & Zsoldos, E. 1992, A&A, 263, 123

Perrin, G., Ridgway, S. T., Coudé du Foresto, V., Mennesson, B., Traub, W. A., & Lacasse, M. G. 2004, A&A, 418, 675

Rayner, J. T., Toomey, D. W., Onaka, P. M., Denault, A. J., Stahlberger, W. E., Vacca, W. D., Cushing, M. C., & Wang, S. 2003, PASP, 115, 362

Richter, H., Wood, P. R., Woitke, P., Bolick, U., & Seldmayr, E. 2003, A&A, 400, 319

Ridgway, S. T., Carbon, D. F., Hall, D. N. B., & Jewell, J. 1984, ApJS, 54, 177

Rudy, R. J., Dimpfl, W. L., Lynch, D. K., Mazuk, S., Venturini, C. C., Wilson, J. C., Puetter, R. C., & Perry, R. B. 2003, ApJ, 596, 1229

Rushton, M. T., et al. 2005, MNRAS, 360, 1281

Sanford, R. F. 1952, ApJ, 116, 331

Sargent, W. L. W. 1961, ApJ, 134, 142

Schuster, M. T., Humphreys, R. M., & Marengo, M. 2006, AJ, 131, 603

Sheffer, Y. 1993, Ph.D. thesis, Univ. Texas

Sheffer, Y., & Lambert, D. L. 1986, PASP, 98, 914

———. 1987, PASP, 99, 1277

Skuljan, L., & Cottrell, P. L. 2002, MNRAS, 335, 1133

Takeda, Y., & Takada-Hidai, M. 1994, PASJ, 46, 395

Tenenbaum, E. D., et al. 2005, AJ, 130, 256

Thompson, R. I., & Boroson, T. A. 1977, ApJ, 216, L75

Tsuji, T. 1988, A&A, 197, 185

———. 2001, A&A, 376, L1

Vacca, W. D., Cushing, M. C., & Rayner, J. T. 2003, PASP, 115, 389

Wallace, L., & Hinkle, K. 1996, ApJS, 107, 312

———. 1997, ApJS, 111, 445

———. 2002, AJ, 124, 3393

Whitney, C. A. 1962, ApJ, 136, 674

Wilson, J. C., et al. 2001, PASP, 113, 227

Winters, J. M., Keady, J. J., Gauger, A., & Sada, P. V. 2000, A&A, 359, 651

Woitke, P., Goeres, A., & Sedlmayr, E. 1996, A&A, 313, 217

Zsoldos, E., & Percy, J. R. 1991, A&A, 246, 441